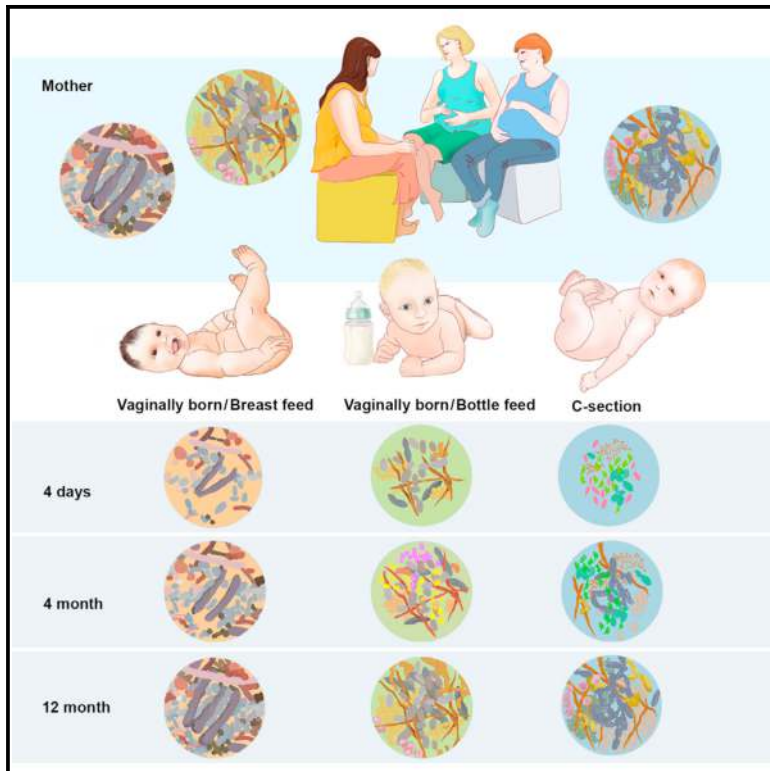


# Cell Host & Microbe

## Dynamics and Stabilization of the Human Gut Microbiome during the First Year of Life

### Graphical Abstract



### Authors

Fredrik Bäckhed, Josefine Roswall, ...,  
Jovanna Dahlgren, Wang Jun

### Correspondence

fredrik.backhed@wlab.gu.se (F.B.),  
jovanna.dahlgren@vgregion.se (J.D.),  
wangj@genomics.org.cn (W.J.)

### In Brief

Bäckhed et al. assessed the gut microbiomes of 98 Swedish mothers and their infants during the first year of life. Cessation of breast-feeding was identified as a major factor in determining gut microbiota maturation, with distinct shifts in signature species being hallmarks of its functional maturation.

### Highlights

- Gut microbiomes of 98 mothers and their infants during the first year of life was assessed
- Cessation of breast-feeding drives the maturation of the infant gut microbiome
- Shifts in signature species demonstrate nonrandom transitions in the infants' gut
- Changes in nutrient and xenobiotic metabolism mark maturation of the gut microbiome

### Accession Numbers

ERP005989



# Dynamics and Stabilization of the Human Gut Microbiome during the First Year of Life

Fredrik Bäckhed,<sup>1,2,\*</sup> Josefine Roswall,<sup>3,4</sup> Yangqing Peng,<sup>5</sup> Qiang Feng,<sup>5,6</sup> Huijue Jia,<sup>5</sup> Petia Kovatcheva-Datchary,<sup>1</sup> Yin Li,<sup>5</sup> Yan Xia,<sup>5</sup> Hailiang Xie,<sup>5</sup> Huanzi Zhong,<sup>5</sup> Muhammad Tanweer Khan,<sup>1</sup> Jianfeng Zhang,<sup>5</sup> Junhua Li,<sup>5</sup> Liang Xiao,<sup>5</sup> Jumana Al-Aama,<sup>5,7</sup> Dongya Zhang,<sup>5</sup> Ying Shiuan Lee,<sup>1</sup> Dorota Kotowska,<sup>6</sup> Camilla Colding,<sup>6</sup> Valentina Tremaroli,<sup>1</sup> Ye Yin,<sup>5</sup> Stefan Bergman,<sup>4,8</sup> Xun Xu,<sup>5</sup> Lise Madsen,<sup>6,9</sup> Karsten Kristiansen,<sup>5,6</sup> Jovanna Dahlgren,<sup>4,12,\*</sup> and Wang Jun<sup>5,6,7,10,11,12,\*</sup>

<sup>1</sup>The Wallenberg Laboratory, Department of Molecular and Clinical Medicine, University of Gothenburg, 41345, Gothenburg, Sweden

<sup>2</sup>Novo Nordisk Foundation Center for Basic Metabolic Research, Section for Metabolic Receptology and Enteroendocrinology, Faculty of Health Sciences, University of Copenhagen, 2200 Copenhagen, Denmark

<sup>3</sup>Department of Pediatrics, Hallands Hospital Halmstad, 30185 Halmstad, Sweden

<sup>4</sup>Göteborg Paediatric Growth Research Center, Department of Paediatrics, the University of Gothenburg, Queen Silvia Children's Hospital, 416 85 Gothenburg

<sup>5</sup>BGI-Shenzhen, Shenzhen 518083, China

<sup>6</sup>Department of Biology, University of Copenhagen, Ole Maaløes Vej 5, 2200 Copenhagen, Denmark

<sup>7</sup>Princess Al Jawhara Albrahim Center of Excellence in the Research of Hereditary Disorders, King Abdulaziz University, Jeddah 21589, Saudi Arabia

<sup>8</sup>Research and Development Center Spenshult, 313 92 Oskarström, Sweden

<sup>9</sup>National Institute of Nutrition and Seafood Research, N-5817 Bergen, Norway

<sup>10</sup>Macau University of Science and Technology, Avenida Wai long, Taipa, Macau 999078, China

<sup>11</sup>Department of Medicine and State Key Laboratory of Pharmaceutical Biotechnology, University of Hong Kong, 21 Sassoon Road, Hong Kong

<sup>12</sup>Co-senior author

\*Correspondence: [fredrik.backhed@wlab.gu.se](mailto:fredrik.backhed@wlab.gu.se) (F.B.), [jovanna.dahlgren@vgregion.se](mailto:jovanna.dahlgren@vgregion.se) (J.D.), [wangj@genomics.org.cn](mailto:wangj@genomics.org.cn) (W.J.)

<http://dx.doi.org/10.1016/j.chom.2015.04.004>

## SUMMARY

The gut microbiota is central to human health, but its establishment in early life has not been quantitatively and functionally examined. Applying metagenomic analysis on fecal samples from a large cohort of Swedish infants and their mothers, we characterized the gut microbiome during the first year of life and assessed the impact of mode of delivery and feeding on its establishment. In contrast to vaginally delivered infants, the gut microbiota of infants delivered by C-section showed significantly less resemblance to their mothers. Nutrition had a major impact on early microbiota composition and function, with cessation of breast-feeding, rather than introduction of solid food, being required for maturation into an adult-like microbiota. Microbiota composition and ecological network had distinctive features at each sampled stage, in accordance with functional maturation of the microbiome. Our findings establish a framework for understanding the interplay between the gut microbiome and the human body in early life.

## INTRODUCTION

The human gut microbiota is an important environmental factor for human health (Clemente et al., 2012), having evolutionarily conserved roles in the metabolism, immunity, development, and behavior of the host (Cabreiro and Gems, 2013; Erkosar

et al., 2013). Although considerable efforts have focused on cataloguing the adult human gut microbiome and its relationship to complex diseases (Human Microbiome Project Consortium, 2012; Karlsson et al., 2013; Li et al., 2014; Qin et al., 2010, 2012), studies on the infant gut microbiota have been restricted to culture-based enumeration, 16S-based profiling, and/or small sample sizes (Adlerberth et al., 2006; Brook et al., 1979; Dominguez-Bello et al., 2010; Eggesbø et al., 2011; Koenig et al., 2011; Palmer et al., 2007; Subramanian et al., 2014; Yatsunenkov et al., 2012). Thus, factors that shape the gut microbiota in early infancy have not been satisfactorily examined.

From an ecological point of view, colonization of the infant's gut represents the de novo assembly of a microbial community (Costello et al., 2012) and is influenced by dietary and medical factors (Eggesbø et al., 2011; Koenig et al., 2011; La Rosa et al., 2014). However, it is not clear how these factors contribute to the overall composition and function of the infants' gut microbiome, and how different microbes cooperate or compete with one another as the gut environment changes.

Here we performed metagenomic shotgun sequencing on fecal samples from 98 full-term Swedish infants and their mothers, assembled gut microbial genomes, and demonstrated gut microbiome signatures characteristic to each chronological and functional stage during the first year of life. In addition, we produced a gene catalog of the developing microbiome, which may constitute an important research tool.

## RESULTS

### Genomes Assembled from the Infants' Gut Microbiome

To characterize the infant gut microbiome, we shotgun-sequenced stool samples from 98 mothers at delivery after a

**Table 1. Descriptive Data of the Study Population, n = 98, Given as Median, Interquartile Ranges, or Percentage**

Mother's age (years)	31	(28–35)	
Mother's prepregnancy weight (kg)	68.5	(59–74)	
Gestational age (days)	281	(275–287)	
Birth weight (gram)	3,620	(3,382–3,995)	
Birth length (cm)	51	(50–52)	
Sampling time mother (days after birth)	2	(0–5)	
Sampling time infant first week (days after birth)	3	(2–5)	
Sampling time infant 4 months (days after birth)	122	(119–125)	
Sampling time infant 12 months (days after birth)	366	(363–372)	
C-section (%)	15.3		
SGA/LGA (%)	2/5.1		
Antibiotics to mother during labor (%)	13.3		
Antibiotics to mother per operative during C-section (%)	11.2		
		First Week	4 Months
Exclusively breast-fed (%)	74.4	68.8	
Mixed fed (formula + breast-feeding) (%)	24.4	19.8	
Exclusively formula-fed (%)	1.2	11.4	
Any breast-feeding (%)	98.8	88.6	14
Antibiotics to infant (first week, 1 week to 4 months, 4–12 months) (%)	2	3	24.5

See also [Table S1](#).

normal pregnancy, and from their infants (15 of whom were delivered by C-section) sampled longitudinally during the first days of life and at 4 and 12 months of age ([Table 1](#) and see [Table S1](#) available online). All infants were born term at gestational age 37–42 weeks, and the majority of parents were of Swedish origin (12/98 infants had at least one parent of non-Swedish origin). In total, we generated 1.52 Tb paired-end reads of high-quality sequences (average 3.99 Gb per sample) ([Table S2](#)). A gene catalog was constructed for each time point based on de novo assembly and metagenomic gene prediction, and functionally annotated using the Kyoto Encyclopedia of Genes and Genomes (KEGG) database ([Table S2](#)).

To structurally organize and taxonomically annotate the genes from the infant samples, we devised a strategy to reconstitute most bacterial or archaeal genomes in their gut metagenome ([Figure S1](#)). We assembled a total of 4,356 genomes (>0.9 MB) de novo, by binning assembled contigs according to abundance variations across samples (similar to construction of metagenomic linkage groups; [Qin et al., 2012](#)). These de novo assembled genomes were complemented by 1,147 genomes from the National Center for Biotechnology Information (NCBI) Bacteria/Archaea genome database. All genomes were subsequently

clustered into 690 unique metagenomic operational taxonomic units (MetaOTUs) that were equivalent to species-level classifications ([Figure S1](#)). Firmicutes and Bacteroidetes were the most prevalent phyla, followed by Actinobacteria and Proteobacteria ([Figure 1A](#)). A total of 373 MetaOTUs were annotated to species ([Table S2](#)); the remaining 317 represented novel species related to known species ([Figure 1A](#)). Although not as complete as the genomes from NCBI, the novel MetaOTUs showed good coverage of conserved single-copy genes (78.6% versus 55.2% on average; [Table S2](#)) ([Rinke et al., 2013](#)). Most of the MetaOTUs constructed from the infant samples were also found in the mothers, where they often showed increased abundance ([Figure 1A](#)).

Principal coordinate analysis (PCoA; unweighted UniFrac distance) ([Lozupone and Knight, 2005](#)) based on the MetaOTUs showed that the samples clustered according to age, and demonstrated that the 12-month-old infant samples were most similar to the mothers ([Figures 1B and 1C](#)). We observed increased  $\alpha$ -diversity but reduced  $\beta$ -diversity as a function of time ([Figure 1D](#)), indicating a more complex and less heterogeneous community. The rising complexity was also supported by increased numbers of microbial genomes identified in the older infants ([Table S2](#)).

#### Inheritance of the Mother's Gut Microbiome

The mode of delivery strongly affected microbiome species in neonates ([Figures S2A and S2B](#); [Table S3](#)). Compared with vaginally born infants, the C-section fecal microbiome was enriched in MetaOTUs such as *Enterobacter hormaechei*/*E. cancerogenus*, *Haemophilus parainfluenzae*/*H. aegyptius*/*H. influenzae*/*H. haemolyticus*, *Staphylococcus saprophyticus*/*S. lugdunensis*/*S. aureus*, *Streptococcus australis* and *Veillonella dispar*/*V. parvula* ([Table S3](#)), indicating that skin and oral microbes, but also bacteria from the surrounding environment during delivery, were the first colonizers in these infants. In contrast, the gut microbiota of vaginally delivered newborns were enriched in microbes from the genera *Bacteroides*, *Bifidobacterium*, *Parabacteroides*, *Escherichia/Shigella* ( $p < 0.05$ ), which also were the most abundant members of the newborns' gut microbiota ([Table S3](#)). However, newborns with *Escherichia/Shigella* as the most abundant genus were sampled earlier than those dominated by *Bacteroides* or *Bifidobacterium* ([Figure S2D](#); on average 2.6, 3.6, and 5.4 days after birth, respectively), in agreement with high abundance of *Escherichia* DNA in the meconium and the placenta ([Aagaard et al., 2014](#); [Gosalbes et al., 2013](#)). Thus, the low abundance of *Escherichia/Shigella* in neonates delivered by C-section could reflect slightly later sampling compared with the vaginally born newborns ( $4.9 \pm 1.9$  versus  $3.6 \pm 2.8$  days after birth). The difference between delivery modes gradually decreased at 4 months and then 12 months of age, but the C-section infants remained more heterogeneous compared to the vaginally born infants ([Figures S2A and S2B](#)). *Bacteroides*, in particular *B. ovatus*/*B. xylanisolvens*, *B. thetaiotaomicron*, *B. uniformis*, and *B. vulgatus*/*B. dorei*, were less prevalent or missing in the C-section-delivered newborns compared to vaginally born infants, and this difference remained at 4 and 12 months ([Table S3](#)).

To investigate to what extent the mothers' gut microbiota contributed to the establishment of the gut microbiota in their infants, we compared the microbial species in newborns and

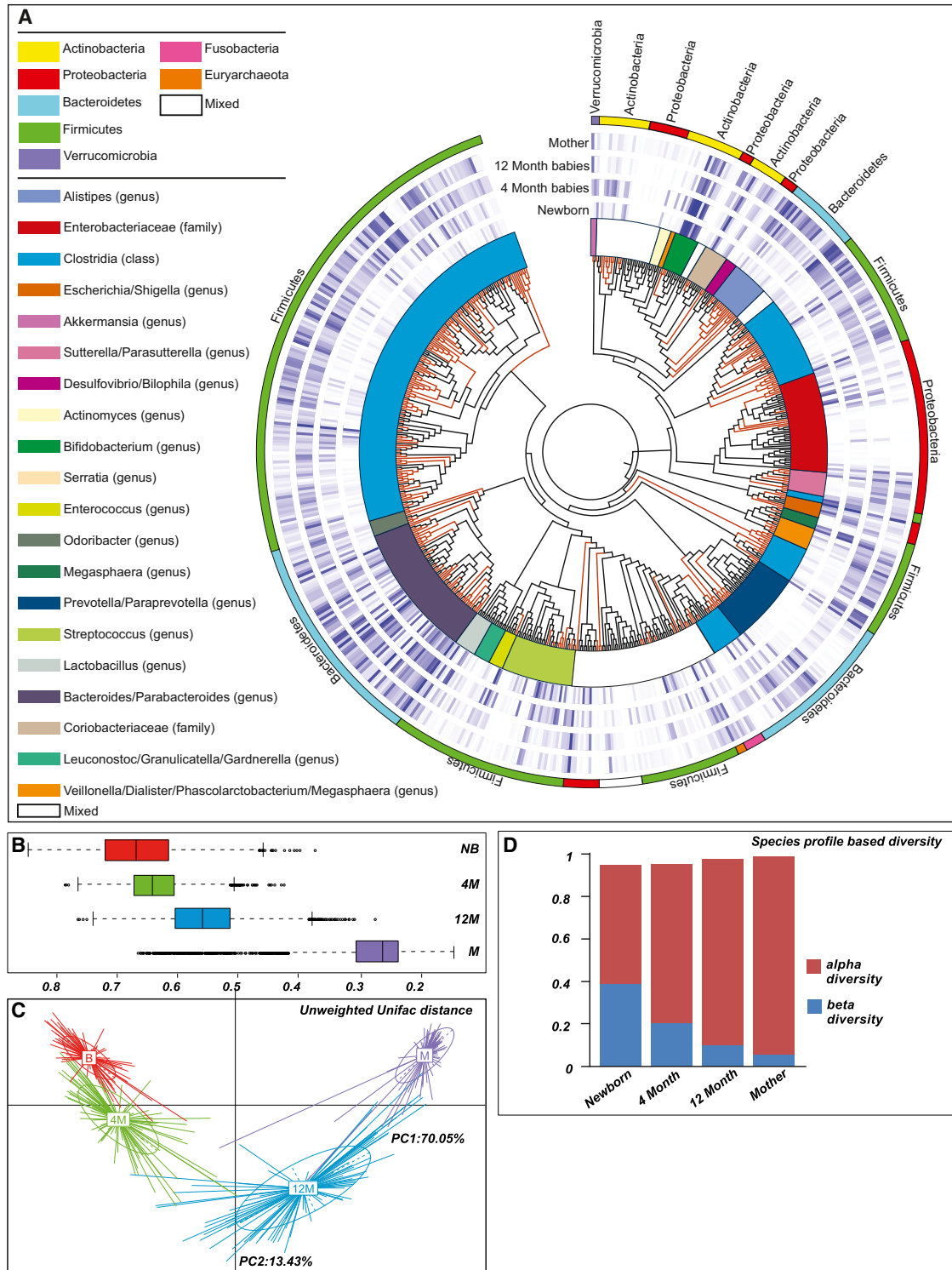


**Figure 1. Phylogenetic Tree of the MetaOTUs and Differences in the Fecal Microbial Communities of Newborns, 4-Month-Old and 12-Month-Old Infants, and Mothers**

(A) Phylogenetic tree constructed from the 625 MetaOTUs present in at least one sample (among the 690 MetaOTUs constructed, 65 showed zero abundance, i.e., all genomes in the MetaOTU have  $L_2/(L_2+L_0) < 0.005$  in all samples according to mapped reads [Supplemental Experimental Procedures]). Averaged genome-genome MUMI distance of MetaOTU pairs was used to construct the tree according to the neighbor-joining method. Novel MetaOTUs are shown as red branches. Colored blocks of outermost circle indicate phyla and of the inner circle indicate genera except Enterobacteriaceae, Clostridia, and Coriobacteriaceae (family). The heatmap circles show relative abundance of each MetaOTU in the newborns, 4-month-old infants, 12-month-old infants, and mothers.

(legend continued on next page)

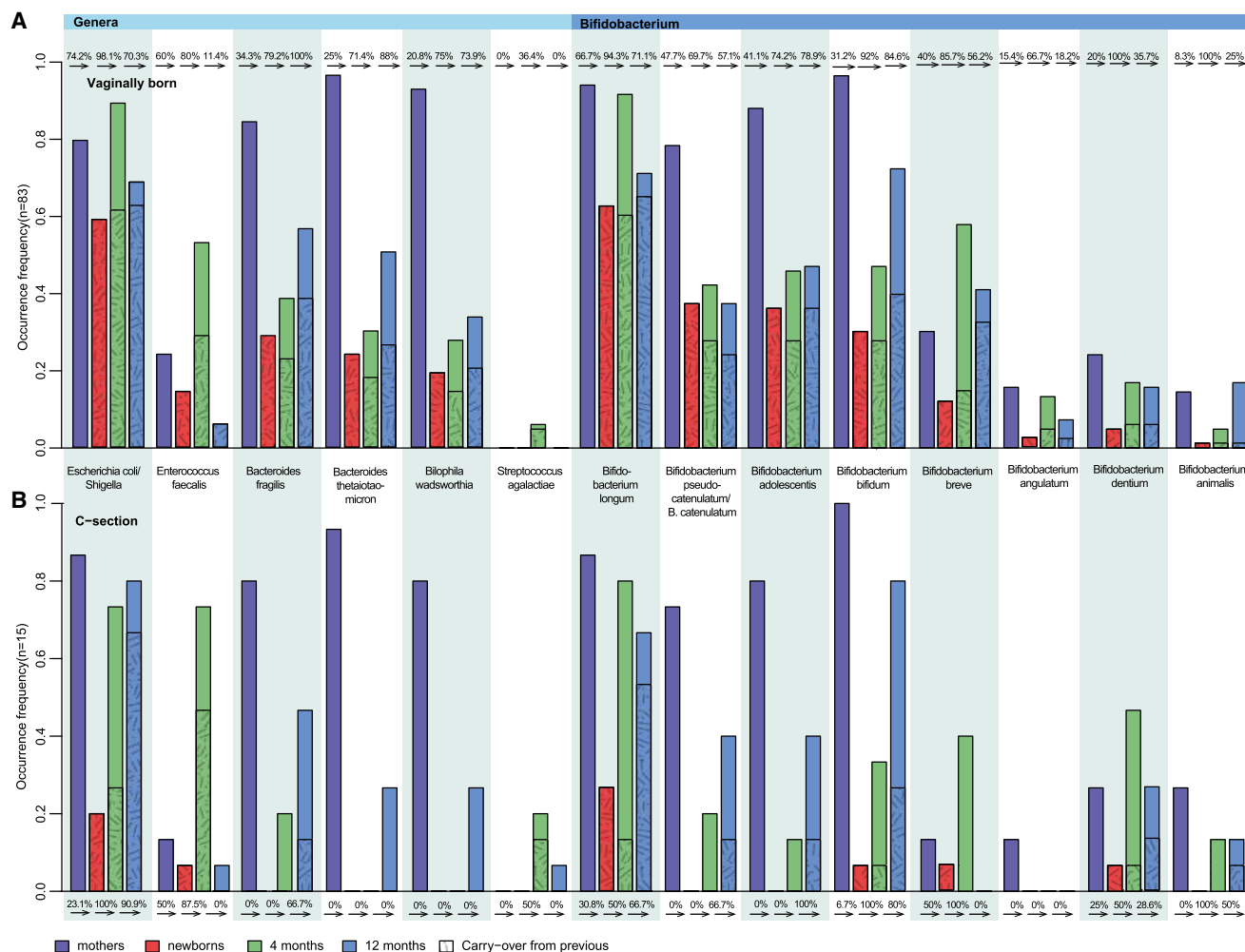


**Figure 2. Compromised Resemblance to the Mother's Gut Microbiome in C-Section Infants**

Occurrence frequency of selected MetaOTUs in the different stages for vaginally born (A) and C-section (B) infants. Within each bar, the hatches mark the part shared with the previous stage, i.e., newborns with their own mothers, 4 month samples with their corresponding newborn samples, 12 month samples with their corresponding 4 month samples. The percentage of such possible carryovers is indicated on the arrows. See also [Figure S2](#) and [Table S3](#).

their mothers. For the 187 taxonomically annotated MetaOTUs present in vaginally delivered newborns, 135 were found in their own mothers ([Table S3](#)), including important species such as *Escherichia/Shigella*, *Bifidobacterium longum*, *Enterococcus faecalis*, *Bacteroides fragilis*, *B. thetaiotaomicron*, *Bilophila wadsworthia* ([Figure 2A](#)), suggesting vertical mother-neonate transfer. The remaining 52 MetaOTUs were not observed in mothers, showed a low prevalence in the newborns (42 MetaOTUs observed in fewer than 5 newborns), and often failed to be transmitted to the 4-month-old infants ([Table S3](#)). A few MetaOTUs found in more than 10 newborns were not found in their mothers, including *Propionibacterium acnes*, *Streptococcus agalactiae*,

and *Veillonella\_oral\_taxon\_780* ([Figure 2A](#); [Table S3](#)), and possibly originated from other body sites or the environment. However, the prevalence of those species declined with age and was completely depleted at 12 months, probably reflecting reduced fitness to persist in the human gut.

Mother-to-infant transmission was compromised in C-section-delivered neonates. We found that 72% (135/187) of the early colonizers of the vaginally delivered newborns' gut matched species found in the stool of their own mother, whereas 41% (55/135) of these species were detected in C-section newborns. We observed less frequent sharing of bacteria such as *Bacteroides*, while sharing of bacteria such as *Enterococcus faecalis* was

(B) Boxplot for unweighted UniFrac distance between the infants' and mothers' MetaOTU profiles (NB, newborn; 4M, 4-month-old infants; 12M, 12-month-old infants; M, mother).

(C) Scatterplot from PCoA, based on unweighted UniFrac distance of the MetaOTUs in each sample.

(D)  $\alpha$ -diversity and  $\beta$ -diversity determined by Rao's diversity decomposition at the MetaOTUs level, considering both phylogeny and relative abundance. See also [Figure S1](#) and [Table S2](#).

retained (Figure 2B; Table S3). Mother-newborn transmission of *Bifidobacterium* was also observed in C-section delivered infants, but with lower frequency compared with vaginally delivered newborns (Table S3), and in agreement with previous studies (Makino et al., 2013). Our results indicate that most of the early colonizers of the newborn gut originate from the mother and that the mode of birth is an important factor shaping the gut microbiota of term infants in early life.

### Functional Maturation of the Gut Microbiome

To determine how the functional capacity of the infant gut microbiota developed during the first year of life, we analyzed the gut microbiome of vaginally delivered infants using the KEGG orthology groups (KOs). During the first year of life the newborn's relatively simple gut microbiome evolved into a more complex and adult-like configuration, consistent with previous studies (Yatsunenkov et al., 2012). We observed increased functional similarity with the mother's gut metagenome and reduced interindividual differences for the 1-year samples (Figure S3A).

The human gut microbiota is a reservoir for antibiotic resistance genes, known as the resistome (Forsslund et al., 2013; Hu et al., 2013; Li et al., 2014). Here we observed the presence of antibiotic resistance genes already in the newborn microbiome (Figures S4A–S4C), possibly a consequence of the relative high abundance of Proteobacteria DNA, whose genomes contain high levels of antibiotic resistance genes (Hu et al., 2013; Li et al., 2014). The newborn microbiome had over 90% prevalence of genes involved in resistance against bacitracin, tetracycline, and macrolides (Figure S4C), the resistance against which were also most prevalent in the adult gut (Forsslund et al., 2013; Hu et al., 2013). Prevalence for resistance against antibiotics such as kanamycin increased with age, with the highest occurrence in the mother microbiome (Figure S4C). Five of the infants received antibiotic treatment within 4 months after delivery, which resulted in a minor shift in the microbiota composition at 4 months (Table S10) but did not affect the pool of antibiotic resistance genes in the 12 months microbiome (Figures S4A and S4B). The microbiome of infants delivered by C-section, however, tended to contain a greater portion of antibiotic resistance genes compared to vaginally delivered infants (Figure S4D, Wilcoxon rank-sum test,  $p = 0.027$  between newborns,  $p = 0.161$  between 4 month olds,  $p = 0.088$  between 12 month olds,  $p = 0.099$  between mothers).

The metagenomic analyses also revealed distinct energy source utilization in the infant gut at the sampled time points (Table S4). In particular, phosphotransferase system (PTS) genes for carbohydrate uptake were enriched in the newborn microbiome, while the lactose-specific transporter was most abundant in 4-month-old infants (Figures 3A and 3B), consistent with a diet dominated by milk. The microbiomes of newborns and 4-month-old infants were enriched in genes required for degradation of sugars from the breast milk, the major source of nutrition in these two groups. In contrast,  $\beta$ -glucoside-specific transporters were most abundant in the 4-month-old and 12-month-old infants (Figure 3B). Accordingly, the 12-month microbiome was enriched in genes involved in degradation of complex sugars and starch (Figure 3A) and associated with increased abundance of *B. thetaiotaomicron* (Figure S3B), known to have a wide repertoire of glycan-degrading enzymes (Sonnenburg

et al., 2005; Xu and Gordon, 2003), and of modules involved in carbohydrate metabolism (Figures S3C and S3D). The abundance of *B. thetaiotaomicron* and pectinesterase, the primary enzymes in pectin degradation, were most abundant in the 12 months infants (Figures S3B and S3C), possibly due to the increased intake at this age of solid or semisolid food rich in pectin at this age.

As a result of the succession of bacterial metabolic functions in the maturing infant gut, we observed that *Desulfovibrio* spp. and *Methanobrevibacter smithii* were abundant in mothers and absent in infants, except in two 12-month-old infants that were colonized by *M. smithii* (Figure S3E). This finding is in agreement with the microbiome's increased capacity for methane production in the mothers (Figures 3A and Figure S3F), which is associated with increased fermentative capacity in the adult microbiome that requires disposal of hydrogen as methane or other byproducts (Charalampopoulos and Rastall, 2009).

The microbiome is exposed to a larger variety of dietary substrates as the infant grows older, which is linked to enrichment of genes in the central carbon metabolism (Figure 3A). For example, KO modules for pyruvate metabolism, the pyruvate:ferredoxin oxidoreductase catalyzing the conversion of pyruvate to acetyl-CoA, was enriched in 4-month-old and 12-month-old infants versus neonates (Figure S3D). In contrast, the relatively oxidized gut environment of neonates enables gut microbes to exploit TCA cycle for energy production and metabolism, as shown by the enrichment of KO modules for TCA cycle in neonates compared with 4-month-old and 12-month-old infants and the mothers (Figure S3D). Taken together, our results indicate that the microbiome adapts to the availability of energy substrates as the infant grows older.

The gut microbiome is an important producer of vitamins (Figures 3A, S3G, and S3H). All newborns in Sweden receive prophylactic vitamin K injections to avoid classic hemorrhagic disease. We observed enriched levels of genes for vitamin K2 (menaquinone) synthesis in newborns, which correlated with the high abundance of *Bacteroides* and *Escherichia/Shigella* (Table S4), known vitamin K2 producers (Wang et al., 2013). Vitamin K2 is important for bone and heart health, and the microbiome was recently described to modulate bone homeostasis (Sjögren et al., 2012). Metabolism of retinol was also most enriched in the newborns (Figure S3H), with implications in several essential developmental processes such as vision, bone, and teeth. Vitamins from the so-called B complex are needed for the body to convert nutrients into glucose and produce energy. Folate (vitamin B9) is one of the essential B vitamins involved in DNA synthesis and repair. Folate biosynthetic genes were significantly enriched in newborns (Figures 3A, S3G, and S3H). Genes for pyridoxal (vitamin B6) and biotin (vitamin B7) synthesis were also significantly enriched in newborns. In contrast, thiamine, pantothenate and cobalamin (vitamins B1, B5, and B12, respectively) biosynthetic genes increased with age, consistent with a previous study (Yatsunenkov et al., 2012) (Figures S3G and S3H). However, modules for vitamin B12 transport system were strongly increased in the newborn metagenome, but decreased with age (Table S4). Similarly, transporters for iron, hemin, and heme, which are linked to vitamin B12 synthesis and important for iron metabolism, were also increased in the microbiome of newborns (Figure S3I).

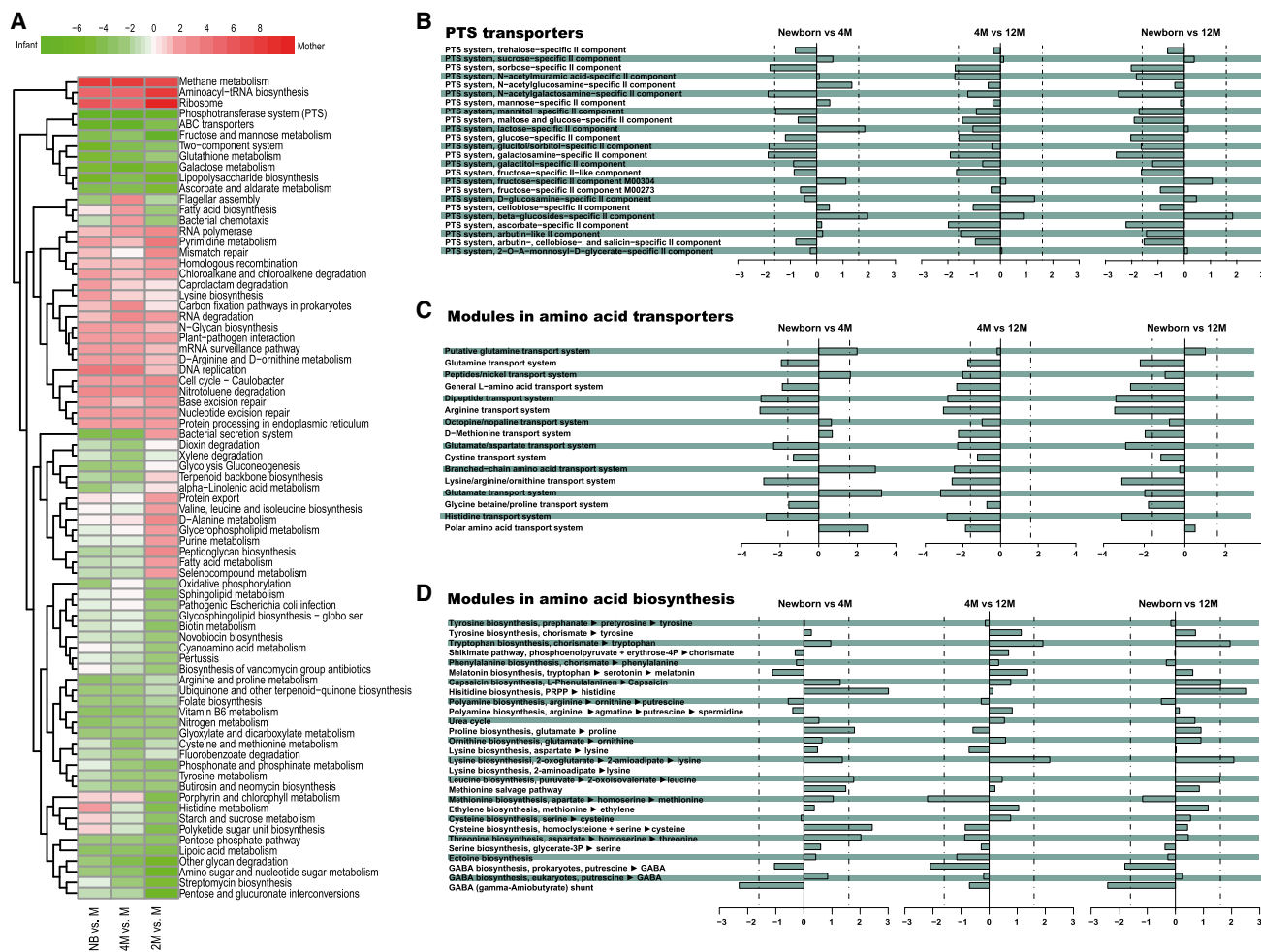


**Figure 3. Functional Maturation of the Fecal Microbiota in Vaginally Born Infants during the First Year of Life**

(A) Heatmap and hierarchical clustering of KO pathways enriched in the metagenome of the newborn (NB), 4-month-old infants (4M), or 12-month-old (12M) infants compared with their mothers (M). KO pathways with a greater than 1.6 reporter score in at least one cohort are plotted.

(B–D) Reporter score barplot comparing abundance of phosphotransferase systems (PTS) transporter modules (B), amino acid transporters (C), or amino acid biosynthesis modules (D) in vaginally born infants ( $n = 81$  for newborns,  $n = 83$  for 4-month-old infants, 12-month-old infants, and mothers). Only modules with more than 40% of KOs found in the metagenomes are shown. Dashed lines represent the reporter score of 1.6, the threshold for a significant difference used in such analyses (Supplemental Experimental Procedures). See also Figures S3 and 4 and Table S4.

The representation of KOs for amino acid metabolism also varied with age (Figures 3A, 3C, and 3D; Table S4). The transport systems for all essential amino acids were increased in the neonate's microbiome, and the levels remained high until the age of 4 months (Figure 3C). Protein requirements, calculated per kilogram of body weight, gradually decrease with age until weaning (Boudry et al., 2010), which in parallel could affect the requirement for amino acids transport systems in agreement with our data. The pathway or modules for methionine degradation, lysine biosynthesis, leucine, and tryptophan metabolism increased with time and reached levels comparable to those found in the mothers by 12 months of age (Figures 3A and 3D; Table S4). Finally, the genes for synthesis and metabolism of the amino acid neurotransmitter GABA (gamma-aminobutyrate) and the hormone melatonin showed differential enrichment in neonates, 4 month olds, and 12 month olds (Figure 3D). In humans, melatonin

plays a role in entraining the circadian system (Reiter, 1991). The fact that newborns do not have an established circadian melatonin rhythm, which appears later, at 3–4 months of age, and matures in childhood, concurs with our observation on melatonin biosynthesis fluctuation (Ardura et al., 2003).

### Signature Taxa at Each Stage

Next we characterized distinctive features of the first year's gut microbiome and defined signature taxa in vaginally and C-section-delivered infants using an established ecology method that considers both the abundance and the prevalence of different taxa (Dufrene and Legendre, 1997). In the vaginally delivered group, newborns harbored bacteria from *Enterococcus*, *Escherichia/Shigella*, *Streptococcus*, and *Rothia* (Figure 4A; Table S5), suggesting a relatively aerobic gut environment. The genera *Bifidobacterium*, *Lactobacillus*, *Collinsella*,

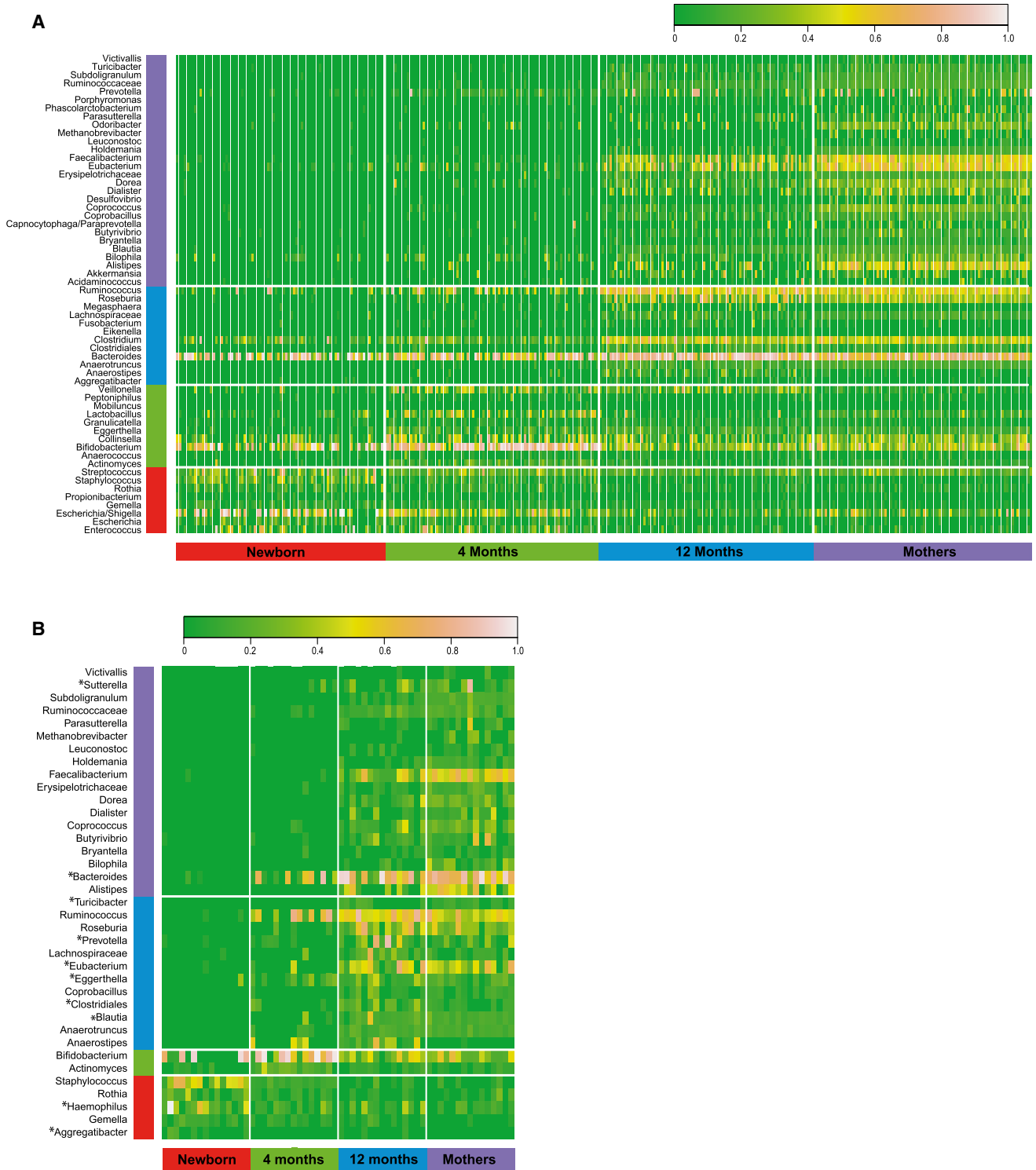


**Figure 4. Dynamics of Signature Genera at Each Stage**

Heatmap of the relative abundance of the signature genera in vaginally (A) or C-section (B) -born infants at birth, after 4 months, after 12 months, and in their mothers (Table S5). Each vertical lane corresponds to one sample. Signature genera only seen in C-section or shifted in different stages compared with vaginally born infants are highlighted with an asterisk. See also Table S5.

*Granulicatella*, and *Veillonella* were identified as signatures of the 4-month microbiome, which indicated reduced oxygen concentration and increased production and utilization of lactic acid for a diet mainly composed of milk (Figure 4A). Signature genera at 12 months included bacteria found in newborns, i.e., *Bacteroides*; bacteria emerging at 4 months, e.g., *Anaerostipes*, *Anaerotruncus*, and *Clostridiales*; and bacteria that only occurred at 12 months, i.e., *Eikenella* (Figure 4A; Table S5). Many of these microbes are efficient degraders of dietary fibers and producers of short chain fatty acids (SCFAs), suggesting a shift toward a more adult-like intestinal environment associated with the increased functional capacity for carbohydrates degradation. The C-section infants (n = 15) appeared to differ from the vaginally delivered infants in signature genera at each stage (Figure 4B; Table S5), e.g., *Blautia* and *Prevotella* were signature at 12 months instead of in the mothers.

Moreover, we also observed that the ecological network was remodeled as the gut microbiota of vaginally delivered infants progressed into an older stage (permutational  $p < 0.05$ ; Figure 5). The relative abundance of MetaOTUs annotated to *Escherichia* and *Staphylococcus* species negatively correlated with each other but became positively correlated in 4 months (Spearman's correlation coefficient  $< -0.6$  in newborn,  $> 0.6$  in 4 months; Figure 5A). A number of facultative anaerobes positively correlated with many obligate anaerobes in newborns but had much reduced or negative correlations at 4 months, likely reflecting decrease in oxygen concentration and more defined ecological niche (Figure 5A). The transition from positive to negative correlation between *Veillonella atypica* and *Peptoniphilus* and *Anaerococcus* species might also indicate increased butyrate instead of lactate production by the *Peptoniphilus* and *Anaerococcus* species (Ezaki et al., 2001) at 4 months. *Bifidobacterium longum*, a signature MetaOTU at 4 months (Table S6), showed such transition from positive to negative correlation with *B. adolescentis* (Figure 5A), suggesting competition or diversifying selection. From 4 to 12 months, *Ruminococcus gnavus* had the greatest number of significantly changed connections (Figure 5B). Both *R. gnavus* and *Roseburia inulinivorans* were signature MetaOTUs of the 12-month-old infants (Table S6). *R. gnavus* can utilize host mucin glycans and has been found to increase in adult patients with Crohn's disease, while *Roseburia inulinivorans* grows on the prebiotic dietary fiber inulin (Joossens et al., 2011; Prindiville et al., 2004; Willing et al., 2010). Collectively, these results indicate that both the composition and the network structure of the gut microbiota evolve as the infants grow, in response to environmental factors and resources feeding into the community.

### Feeding Pattern and Gut Microbial Maturation

To better evaluate the role(s) of different factors on the establishment of the gut microbiota during the first year of life, we analyzed the impact of breast-feeding in vaginally delivered infants. The feeding pattern reported as exclusively breast-feeding or mixed feeding during the first week of life did not significantly affect the newborn microbiome ( $p > 0.05$ , PERMANOVA; Table S7). We evaluated potential differences in gut microbial maturation and chronological age coincident with the different feeding pattern (Figures 6A and 6B). The random forest model (Subramanian et al., 2014) was trained using relative abundances of all

MetaOTUs in exclusively breast-fed newborns (n = 49, who were also vaginally delivered and ceased breast-feeding between 4 and 12 months), and 64 MetaOTUs (27 of which were novel species) were selected as markers for gut microbiota age (Figures 6A and S5A; Table S7). On the test set consisting of infants who as newborns received formula in addition to breast milk, the age estimates at newborn and 4 months were often older compared to the exclusively breast-fed newborns (Figures 6A and 6B). Using the same model we noted that gut microbiota was also older in C-section-delivered infants at birth and at 4 months compared with vaginally delivered infants (Figure S5B).

At 4 months, we noted clear differences between infants who received exclusive breast-feeding and exclusive formula-feeding, respectively, in the gut microbiota at the MetaOTU level (Table S7). Exclusively breast-fed infants had increased levels of taxa that are used as probiotics such as *L. johnsonii/L. gasseri*, *L. paracasei/L. casei*, and *B. longum* (Table S7). Four-month-old formula-fed infants had elevated levels of *Clostridium difficile*, *Granulicatella adiacens*, *Citrobacter spp.*, *Enterobacter cloacae*, *Bilophila wadsworthia*, in agreement with previous studies (Bezirtzoglu et al., 2011; Penders et al., 2005). *B. adolescentis* was enriched in the formula-fed infants, consistent with its positive to negative correlation with *B. longum* from newborn to 4 months (Figure 5). Although the overall functional difference was small (feeding pattern at 4 months accounted for 1.30% of the variation in KOs,  $p = 0.33$ , PERMANOVA; Table S7), formula-fed infants were enriched in KO modules for some of the transporters in the PTS system and enriched in functions found in the adult microbiome, such as bile acid biosynthesis and methanogenesis (Figure 6D; Table S7). According to the CAZy (carbohydrate-active enzymes) database (Lombard et al., 2014), formula-fed infants exhibited an overrepresentation of GH86, GH116, PL1, and PL2, which are  $\beta$ -agarase or  $\beta$ -porphyranase and pectate lyase (Table S7). In contrast, the microbiome of infants that were exclusively breast-fed had higher levels of KO modules involved in oxidative phosphorylation and synthesis of B vitamins such as riboflavin, tetrahydrofolate, and biotin (Figure 6D; Table S7) and GH119 ( $\alpha$ -amylase; Table S7).

The cessation of breast-feeding had profound effects on the microbiota in 12-month-old infants and shifted the microbial ecology toward an adult-like composition enriched in *Bacteroides*, *Bilophila*, *Roseburia*, *Clostridium*, and *Anaerostipes* (Table S7). In contrast, the gut microbiome of infants breast-fed at 12 months was still dominated by *Bifidobacterium*, *Lactobacillus*, *Collinsella*, *Megasphaera*, and *Veillonella* (Table S7), bacteria that have previously been found in breast milk (Jost et al., 2014). Consistently, the "microbiota age" of these 12 month olds appeared younger than that of infants who were no longer breast-fed (compare Figure 6E with Figures 6A and 6B). Thus our results underscore the role of breast-feeding in the shaping and succession of gut microbial communities during the first year of life.

### DISCUSSION

Our study shows how the gut microbiota develops during the first year of life after a normal term pregnancy in 98 full-term Swedish children. Mode of delivery and cessation of breast-feeding were two key factors driving the assembly of an adult-like gut microbiota. We observed nonrandom transitions



microbiota over time, as reported previously from lateral comparison of different children and adults (Yatsunenko et al., 2012). Based on the survey of 16S rRNA, the authors concluded that the infant microbiome gradually matures into an adult-like structure until the age of 3 years (Yatsunenko et al., 2012). However, this might be more based on the gut microbiota in the Malawian and Amerindian children, as the 1-year-old infants from the United States were already as close to the adults as teenagers. In our Swedish cohort, infants at 12 months were more similar to their mothers than were newborn infants or newborns at 4 months. However, differences remained in the gut microbiome between the 1-year-old children and the mothers both compositionally and functionally, awaiting further maturation.

Consistent with a previous study on premature infants (La Rosa et al., 2014), our results show that the maturation of the gut microbiota is a nonrandom process, where distinct signature species and a network of changing positive and negative interactions between key microbial taxa can be identified at each sampled age. However, while in preterm neonates host biology (gestational age at birth) was indicated as the major driver (La Rosa et al., 2014), our results on term infants show that mode of delivery and feeding patterns have major effects on gut microbiota assembly. We observed that most of the early colonizers are derived from the mother, and that in C-section infants vertical mother-infant transmission was less frequent for important intestinal microbes such as *Bacteroides* and *Bifidobacterium*, while sharing of bacteria from skin and mouth was increased, in line with an earlier study (Dominguez-Bello et al., 2010).

Together with the development of an adult-like microbiota, we also followed the maturation of the functional capacity of the infant microbiome. Our results underscore the role of the gut microbiota for the production of essential amino acids and vitamins for the growing infant. While the infant gut microbiota acquired significant capacity to produce amino acids and vitamins after 4 months of life, the increase in transporters capacity indicates that the newborn's microbiome is poised to the upcoming change in the intestinal environment and progression to a mature profile. Intriguingly, considering evidence that the gut microbiota may affect behavior, many functions of the developing gut microbiome linked to the metabolism of vitamins, iron, and amino acids are also required for normal brain development (Lozoff et al., 1987), thus adding to the possibility that the gut microbiota might affect behavior (Diaz Heijtz et al., 2011; Hsiao et al., 2013).

Our results also underscore the role of breast-feeding in the shaping and succession of gut microbial communities during the first year of life. The gut microbiota of children no longer breast-fed was enriched in species belonging to *Clostridia* that are prevalent in adults, such as *Roseburia*, *Clostridium*, and *Anaerostipes*. In contrast, *Bifidobacterium* and *Lactobacillus* still dominated the gut microbiota of breast-fed infants at 12 months of age. The different microbial configuration was also associated with functional shifts, as the increased capacity to degrade polysaccharides promoted by the introduction of solid foods did not become apparent until the infants stopped breast-feeding. Therefore our results strongly suggest that cessation of breast-feeding rather than introduction of solid foods is the major driver in the development of an adult microbiota. Indeed, recent research has shown that breast-feeding as an infant is associated

with the adult microbiota community type (i.e., *Bacteroides*-dominated) (Ding and Schloss, 2014), and with a distinct microbiota profile and expansion of Th17-based immune response in rhesus macaques (Ardeshir et al., 2014). These studies and our results hint to the life-long effects of breast-feeding for the priming of the gut microbiome, with possible effects on metabolic and immune health that we are only beginning to understand.

## EXPERIMENTAL PROCEDURES

### Study Population and Sampling

The study population was recruited before birth upon mothers' arrival to the delivery ward, as part of a larger study (Gerd et al., 2012), and the study was approved by the Regional Ethical Review Board in Lund. Informed consent was obtained from all mothers. Ninety-eight complete infant/mother samples were obtained. The infants (44 boys/54 girls) were all the result of healthy term pregnancies planning vaginal delivery (C-section [ $n = 15$ ], vaginally born [ $n = 83$ ], two newborn samples from vaginally delivered and one newborn delivered through C-section were missing; Table 1). Fecal sample series including mother at birth and infant as newborn, aged 4 (time for introduction of solid foods) and 12 months (when children are generally fed full meals), were collected, and feeding pattern and antibiotic usage were recorded (Supplemental Experimental Procedures). Samples were frozen at  $-80^{\circ}\text{C}$  and stored until further analysis.

### DNA Extraction and Metagenomic Sequencing

Genomic DNA was isolated from approximately 100 mg of stool using the NucleoSpin Soil kit for (MACHEREY-NAGEL, Germany) following the manufacturer's instruction, with the only modification being that the vortex step was replaced with repeated bead beating at 5.5 m/s for 60 s using the FastPrep-24 Instrument (MP Biomedicals).

DNA library construction was performed following the manufacturer's instruction (Illumina HiSeq2000). One paired-end library with insert size of 350 bp for each sample was built and sequenced with 100 bp read length from each end. Adaptor contamination, low-quality reads, and host contaminating reads were removed from the raw sequencing reads sets. On average 39.9 million high-quality reads per sample were generated for further analyses. The proportion of high-quality reads among all raw reads from each sample was 86.7% on average.

### De Novo Assembly of Contigs and Genomes

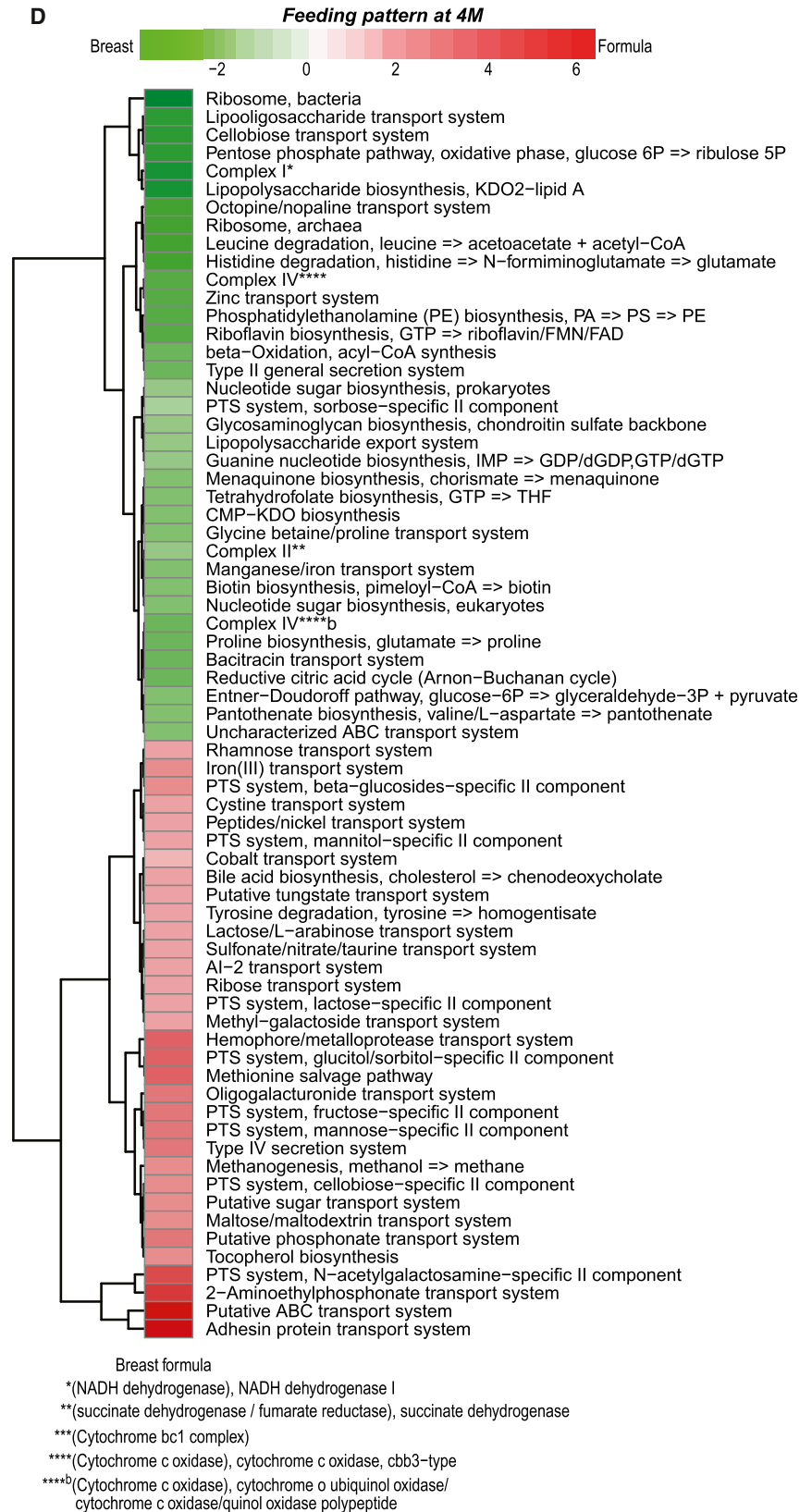
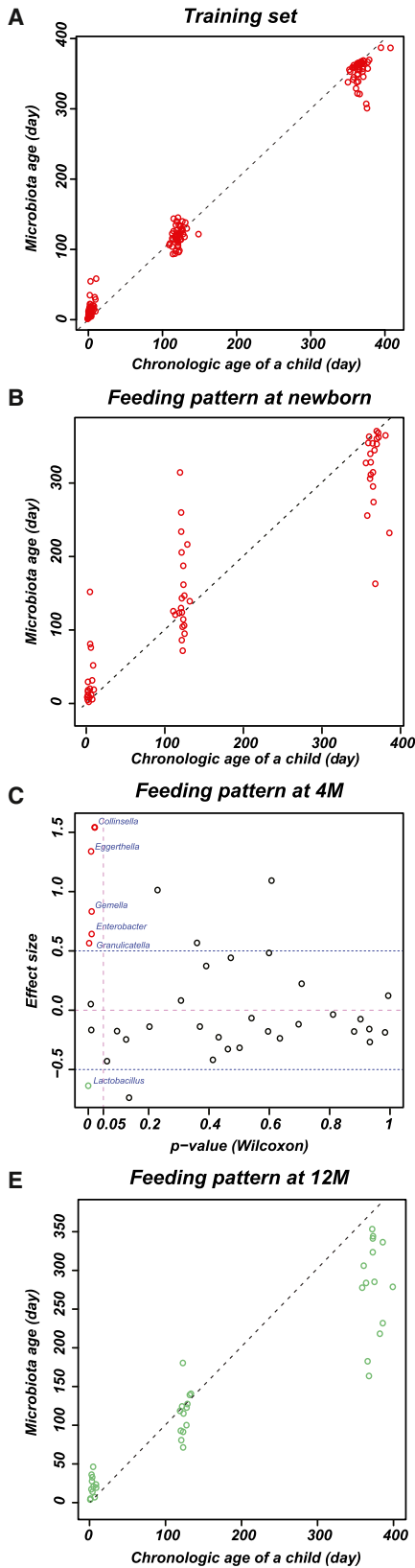
We assembled high-quality reads into contigs for each of the samples using SOAPdenovo2 (Luo et al., 2012). For each sample, contigs that did not map to known genomes in the NCBI database were binned according to their covariations across samples using an Ordering Points to Identify the Clustering Structure (OPTICS) algorithm (Supplemental Experimental Procedures). Each bin was then optimized using an expectation maximization (EM) algorithm and manually curated according to GC content versus depth of coverage (GC-depth) graphs. Contigs within each bin were assembled into genomes using SOAPdenovo2 (Luo et al., 2012).

### Construction of MetaOTUs and Taxonomic Assignments

A total of 4,356 de novo assembled draft genomes and 1,147 bacterial or archaeal genomes from NCBI that were detectable in our samples were clustered into MetaOTUs according to genome-genome distance based on MUMi (Deloger et al., 2009) and the Spearman distance (Leung et al., 2011). The parameters were optimized so that each MetaOTU represents a species (Supplemental Experimental Procedures).

The taxonomic assignment of each MetaOTU is determined by the taxonomic information of the NCBI genomes that resided within the MetaOTU.

All 313 unannotated MetaOTUs and 116 of the 373 annotated MetaOTUs that also contained newly assembled genomes were analyzed by a set of conserved single-copy genes (SCGs, 139 genes for bacteria) as described in Rinke et al. (2013), and coverage of the 139 bacterial genes indicates completeness of the genomes (Table S2). For the 116 MetaOTUs containing both newly assembled genomes and reference genomes from NCBI, the statistics were performed separately for these genomes. Nonredundant genes in



(legend on next page)

the MetaOTUs were aligned to the SCGs by using the Pfam database (default parameters), and the match with the best bit score was used if a gene aligned to multiple SCGs, i.e., unique annotation.

### Gene Catalog Construction and Functional Annotation

We performed gene prediction using GeneMark v2.7 from the assembled contigs (Qin et al., 2010). All predicted genes were aligned pairwise using BLAT (Kent, 2002) and genes, of which over 90% of their length can be aligned to another one with more than 95% identity (no gaps allowed), were removed as redundancies. We constructed four gene catalogs for newborns, 4 month infants, 12 month infants, and the mothers, respectively.

We translated the nonredundant genes into putative amino acid sequences and aligned these genes against a set of protein sequences from KEGG (release 59.0, with animal and plant sequences removed) using BLASTP (e value  $\leq 1e-5$ ). Each protein was assigned to the KO by the highest scoring annotated hit(s) containing at least one HSP scoring over 60 bits. Annotation to glycoside hydrolases (GHs) and polysaccharide lyases (PLs) in the CAZy database (Lombard et al., 2014) were performed by matching their corresponding enzymes (ECs) from the KO results.

Differentially enriched KO pathways, modules, or CAZy families were identified according to their reporter score (Patil and Nielsen, 2005), from the Z scores of individual KOs (Supplemental Experimental Procedures).

### Taxonomic Annotation and Abundance Calculation

Taxonomic assignment of the predicted genes was performed according to the IMG database (v400) using an in-house pipeline detailed previously (Qin et al., 2012), with 70% overlap and 65% identity for assignment to phylum, and 85% identity to genus. The relative abundance of a taxon was calculated from the relative abundance of its genes (Supplemental Experimental Procedures).

### Ecological Parameters

The total diversity in the MetaOTU or KO profile of each cohort was decomposed into  $\alpha$ -diversity (within-sample) and  $\beta$ -diversity (between-sample) according to the method proposed by Rao (Rao, 1984, 1982).

Signature genera or MetaOTUs were identified according to their IndVal values, which consider both the occurrence and abundance of a taxon (Duffrène and Legendre, 1997) (Supplemental Experimental Procedures).

### MetaOTU Networks

Spearman's correlation coefficient was calculated between any two MetaOTUs according to their abundance fluctuations in each stage for the vaginally delivered infants. Changed interactions between newborn and 4 months or between 4 months and 12 months were identified by subtracting the coefficient in one stage from the other (Table S6). MetaOTUs present in less than six samples, or with Spearman's  $\rho$  between  $-0.6$  and  $0.6$ , or  $p \geq 0.05$  in both stages under comparison were not considered. Permutation was performed for 999 times to test whether the change was equal to 0. The percentage of the test statistics not less than the one from the original observation was the permutational  $p$  value. Networks were visualized using Cytoscape 3.0.2.

### Calculation of Gut Microbiota Age

The relative abundance profile of all MetaOTUs in each training sample ( $n = 49$ ) was fit against its corresponding chronological age (unit, days) using default parameters in the randomForest package in R (3.0.1), as was done previously with OTUs from 16S pyrosequencing (Subramanian et al., 2014). According to rfcv function in the random forest package, 64 MetaOTUs led to a reasonably

good fit (Figure S4A), and they ranked top 64 in permutational importance (Table S7). The random model based on these 64 MetaOTUs was then applied to the test samples ( $n = 15, 21, 9$ ) to calculate their "gut microbiota age." Both the chronological age and the gut microbiota age were continuous numbers, as in Subramanian et al. (2014).

### ACCESSION NUMBERS

Gut metagenome sequences have been deposited to EBI's Sequence Read Archive under the accession code ERP005989. Draft genome assemblies and other data will be deposited to GigaDB (<http://gigadb.org/>).

### SUPPLEMENTAL INFORMATION

Supplemental Information includes Supplemental Experimental Procedures, five figures, and seven tables and can be found with this article at <http://dx.doi.org/10.1016/j.chom.2015.04.004>.

### AUTHOR CONTRIBUTIONS

F.B., J.R., and J.D. conceived and designed the project. F.B., K.K., J.D., and W.J. monitored the project. J.R., S.B., and J.D. collected samples. P.K.D., Y.L., D.K., C.C., and V.T. performed experiments. F.B., J.R., Y.P., Q.F., H.J., P.K.D., Y.L., Y.X., H.X., M.T.K., J.Z., J.L., L.X., D.Z., X.X., L.M., J.D., and K.K. analyzed and interpreted the data. F.B., J.R., Y.P., Q.F., H.J., P.K.D., M.T.K., and J.D. wrote the paper. All authors commented on the manuscript.

### ACKNOWLEDGMENTS

We thank the infants and their mothers for participating in this study, Rosie Perkins for editing the manuscript, and Anna Hallén for help with figures. This study was supported by the Knut and Alice Wallenberg Foundation; the Swedish Research Council; the NovoNordisk Foundation; Torsten Söderberg's foundation; IngaBritt och Arne Lundberg's foundation; the Regional Scientific Council of the Southern Health Care Region; the Regional Scientific Council of Halland; and the regional agreement on medical training and clinical research (ALF) between Region Västra Götaland and Sahlgrenska University Hospital, the Natural Science Foundation of China (30890032, 30725008, 3081130531, 31161130357), the Shenzhen Municipal Government of China (BGI20100001, CXB201108250096A, CXB201108250098A, JSJGG20140702161403250, and DRC-SZ[2015]162), the Danish Strategic Research Council grant (2106-07-0021), the Ole Rømer grant from Danish Natural Science Research Council, and the Solexa project (272-07-0196). F.B. is a shareholder in MetaboGen AB.

Received: October 15, 2014

Revised: January 27, 2015

Accepted: April 8, 2015

Published: April 9, 2015

### REFERENCES

Aagaard, K., Ma, J., Antony, K.M., Ganu, R., Petrosino, J., and Versalovic, J. (2014). The placenta harbors a unique microbiome. *Sci. Transl. Med.* **6**, 237ra65.

### Figure 6. Effects of Feeding Pattern on the Microbiome

(A) Microbiota age versus chronological age in the training set ( $n = 49$ , vaginally delivered, exclusive breast-feeding at newborn and cessation of breast-feeding at 12 months).

(B) Microbiota age versus chronological age in a test set comprised of vaginally delivered infants who had mixed feeding as newborns ( $n = 21$ ).

(C) Genera affected by feeding pattern at 4 months (Table S7). Positive effect size, enriched in breast-feeding ( $n = 59$ ); negative effect size, enriched in formula-feeding ( $n = 8$ ).  $p$  value according to Wilcoxon rank-sum test.

(D) KO modules affected by feeding pattern at 4 months (reporter score greater than 1.6; Table S7). Green, enriched in breast-feeding ( $n = 59$ ); red, enriched in formula-feeding ( $n = 8$ ).

(E) Microbiota age versus chronological age in a test set comprised of vaginally delivered infants who were still breast-fed at 12 months ( $n = 12$  for newborn;  $n = 14$  for 4 and 12 months). See also Figure S5 and Table S7.

- Adlerberth, I., Lindberg, E., Aberg, N., Hesselmar, B., Saalman, R., Strannegård, I.-L., and Wold, A.E. (2006). Reduced enterobacterial and increased staphylococcal colonization of the infantile bowel: an effect of hygienic lifestyle? *Pediatr. Res.* *59*, 96–101.
- Ardeshir, A., Narayan, N.R., Mendez-Lagares, G., Lu, D., Rauch, M., Huang, Y., Van Rompay, K.K., Lynch, S.V., and Hartigan-O'Connor, D.J. (2014). Breast-fed and bottle-fed infant rhesus macaques develop distinct gut microbiotas and immune systems. *Sci. Transl. Med.* *6*, 252ra120–ra252ra120.
- Ardura, J., Gutierrez, R., Andres, J., and Agapito, T. (2003). Emergence and evolution of the circadian rhythm of melatonin in children. *Horm. Res.* *59*, 66–72.
- Bezirtoglou, E., Tsiotsias, A., and Welling, G.W. (2011). Microbiota profile in feces of breast- and formula-fed newborns by using fluorescence in situ hybridization (FISH). *Anaerobe* *17*, 478–482.
- Boudry, G., David, E.S., Douard, V., Monteiro, I.M., Le Huërou-Luron, I., and Ferraris, R.P. (2010). Role of intestinal transporters in neonatal nutrition: carbohydrates, proteins, lipids, minerals, and vitamins. *J. Pediatr. Gastroenterol. Nutr.* *51*, 380–401.
- Brook, I., Barrett, C.T., Brinkman, C.R., 3rd, Martin, W.J., and Finegold, S.M. (1979). Aerobic and anaerobic bacterial flora of the maternal cervix and newborn gastric fluid and conjunctiva: a prospective study. *Pediatrics* *63*, 451–455.
- Cabreiro, F., and Gems, D. (2013). Worms need microbes too: microbiota, health and aging in *Caenorhabditis elegans*. *EMBO Mol. Med.* *5*, 1300–1310.
- Charalampopoulos, D., and Rastall, R.A. (2009). *Prebiotics and Probiotics Science and Technology* (New York: Springer).
- Clemente, J.C.C., Ursell, L.K.K., Parfrey, L.W.W., and Knight, R. (2012). The impact of the gut microbiota on human health: an integrative view. *Cell* *148*, 1258–1270.
- Costello, E.K., Stagaman, K., Dethlefsen, L., Bohannan, B.J.M., and Relman, D.A. (2012). The application of ecological theory toward an understanding of the human microbiome. *Science* *336*, 1255–1262.
- Deloger, M., El Karoui, M., and Petit, M.-A. (2009). A genomic distance based on MUM indicates discontinuity between most bacterial species and genera. *J. Bacteriol.* *191*, 91–99.
- Diaz Heijtz, R., Wang, S., Anuar, F., Qian, Y., Björkholm, B., Samuelsson, A., Hibberd, M.L., Forssberg, H., and Pettersson, S. (2011). Normal gut microbiota modulates brain development and behavior. *Proc. Natl. Acad. Sci. USA* *108*, 3047–3052.
- Ding, T., and Schloss, P.D. (2014). Dynamics and associations of microbial community types across the human body. *Nature* *509*, 357–360.
- Dominguez-Bello, M.G., Costello, E.K., Contreras, M., Magris, M., Hidalgo, G., Fierer, N., and Knight, R. (2010). Delivery mode shapes the acquisition and structure of the initial microbiota across multiple body habitats in newborns. *Proc. Natl. Acad. Sci. USA* *107*, 11971–11975.
- Dufrêne, M., and Legendre, P. (1997). Species assemblages and indicator species: the need for a flexible asymmetrical approach. *Ecol. Monogr.* *67*, 345–366.
- Eggesbø, M., Moen, B., Peddada, S., Baird, D., Rugtveit, J., Midtvedt, T., Bushel, P.R., Sekelja, M., and Rudi, K. (2011). Development of gut microbiota in infants not exposed to medical interventions. *APMIS* *119*, 17–35.
- Erkosar, B., Storelli, G., Defaye, A., and Leulier, F. (2013). Host-intestinal microbiota mutualism: “learning on the fly”. *Cell Host Microbe* *13*, 8–14.
- Ezaki, T., Kawamura, Y., Li, N., Li, Z.Y., Zhao, L., and Shu, S. (2001). Proposal of the genera *Anaerococcus* gen. nov., *Peptoniphilus* gen. nov. and *Gallicola* gen. nov. for members of the genus *Peptostreptococcus*. *Int. J. Syst. Evol. Microbiol.* *51*, 1521–1528.
- Forslund, K., Sunagawa, S., Kultima, J.R., Mende, D.R., Arumugam, M., Typas, A., and Bork, P. (2013). Country-specific antibiotic use practices impact the human gut resistome. *Genome Res.* *23*, 1163–1169.
- Gerd, A.-T., Bergman, S., Dahlgren, J., Roswall, J., and Alm, B. (2012). Factors associated with discontinuation of breastfeeding before 1 month of age. *Acta Paediatr.* *101*, 55–60.
- Gosalbes, M.J., Llop, S., Vallès, Y., Moya, A., Ballester, F., and Francino, M.P. (2013). Meconium microbiota types dominated by lactic acid or enteric bacteria are differentially associated with maternal eczema and respiratory problems in infants. *Clin. Exp. Allergy* *43*, 198–211.
- Hsiao, E.Y., McBride, S.W., Hsien, S., Sharon, G., Hyde, E.R., McCue, T., Codelli, J.A., Chow, J., Reisman, S.E., Petrosino, J.F., et al. (2013). Microbiota modulate behavioral and physiological abnormalities associated with neurodevelopmental disorders. *Cell* *155*, 1451–1463.
- Hu, Y., Yang, X., Qin, J., Lu, N., Cheng, G., Wu, N., Pan, Y., Li, J., Zhu, L., Wang, X., et al. (2013). Metagenome-wide analysis of antibiotic resistance genes in a large cohort of human gut microbiota. *Nat. Commun.* *4*, 2151.
- Human Microbiome Project Consortium (2012). Structure, function and diversity of the healthy human microbiome. *Nature* *486*, 207–214.
- Joossens, M., Huys, G., Cnockaert, M., De Preter, V., Verbeke, K., Rutgeerts, P., Vandamme, P., and Vermeire, S. (2011). Dysbiosis of the faecal microbiota in patients with Crohn’s disease and their unaffected relatives. *Gut* *60*, 631–637.
- Jost, T., Lacroix, C., Braegger, C.P., Rochat, F., and Chassard, C. (2014). Vertical mother-neonate transfer of maternal gut bacteria via breastfeeding. *Environ. Microbiol.* *16*, 2891–1904.
- Karlsson, F.H., Tremaroli, V., Nookaew, I., Bergström, G., Behre, C.J., Fagerberg, B., Nielsen, J., and Bäckhed, F. (2013). Gut metagenome in European women with normal, impaired and diabetic glucose control. *Nature* *498*, 99–103.
- Kent, W.J. (2002). BLAT—the BLAST-like alignment tool. *Genome Res.* *12*, 656–664.
- Koenig, J.E., Spor, A., Scalfone, N., Fricker, A.D., Stombaugh, J., Knight, R., Angenent, L.T., and Ley, R.E. (2011). Succession of microbial consortia in the developing infant gut microbiome. *Proc. Natl. Acad. Sci. USA* *108* (Suppl 1), 4578–4585.
- La Rosa, P.S., Warner, B.B., Zhou, Y., Weinstock, G.M., Sodergren, E., Hall-Moore, C.M., Stevens, H.J., Bennett, W.E., Jr., Shaikh, N., Linneman, L.A., et al. (2014). Patterned progression of bacterial populations in the premature infant gut. *Proc. Natl. Acad. Sci. USA* *111*, 12522–12527.
- Leung, H.C.M., Yiu, S.M., Yang, B., Peng, Y., Wang, Y., Liu, Z., Chen, J., Qin, J., Li, R., and Chin, F.Y.L. (2011). A robust and accurate binning algorithm for metagenomic sequences with arbitrary species abundance ratio. *Bioinformatics* *27*, 1489–1495.
- Li, J., Jia, H., Cai, X., Zhong, H., Feng, Q., Sunagawa, S., Arumugam, M., Kultima, J.R., Prifti, E., Nielsen, T., et al.; MetaHIT Consortium; MetaHIT Consortium (2014). An integrated catalog of reference genes in the human gut microbiome. *Nat. Biotechnol.* *32*, 834–841.
- Lombard, V., Golaconda Ramulu, H., Drula, E., Coutinho, P.M., and Henrissat, B. (2014). The carbohydrate-active enzymes database (CAZY) in 2013. *Nucleic Acids Res.* *42* (Database issue), D490–D495.
- Lozoff, B., Brittenham, G.M., Wolf, A.W., McClish, D.K., Kuhnert, P.M., Jimenez, E., Jimenez, R., Mora, L.A., Gomez, I., and Krauskopf, D. (1987). Iron deficiency anemia and iron therapy effects on infant developmental test performance. *Pediatrics* *79*, 981–995.
- Lozupone, C., and Knight, R. (2005). UniFrac: a new phylogenetic method for comparing microbial communities. *Appl. Environ. Microbiol.* *71*, 8228–8235.
- Luo, R., Liu, B., Xie, Y., Li, Z., Huang, W., Yuan, J., He, G., Chen, Y., Pan, Q., Liu, Y., et al. (2012). SOAPdenovo2: an empirically improved memory-efficient short-read de novo assembler. *Gigascience* *1*, 18.
- Makino, H., Kushiro, A., Ishikawa, E., Kubota, H., Gawad, A., Sakai, T., Oishi, K., Martin, R., Ben-Amor, K., Knol, J., and Tanaka, R. (2013). Mother-to-infant transmission of intestinal bifidobacterial strains has an impact on the early development of vaginally delivered infant’s microbiota. *PLoS ONE* *8*, e78331.
- Palmer, C., Bik, E.M., DiGiulio, D.B., Relman, D.A., and Brown, P.O. (2007). Development of the human infant intestinal microbiota. *PLoS Biol.* *5*, e177.
- Patil, K.R., and Nielsen, J. (2005). Uncovering transcriptional regulation of metabolism by using metabolic network topology. *Proc. Natl. Acad. Sci. USA* *102*, 2685–2689.

- Penders, J., Vink, C., Driessen, C., London, N., Thijs, C., and Stobberingh, E.E. (2005). Quantification of *Bifidobacterium* spp., *Escherichia coli* and *Clostridium difficile* in faecal samples of breast-fed and formula-fed infants by real-time PCR. *FEMS Microbiol. Lett.* *243*, 141–147.
- Prindiville, T., Cantrell, M., and Wilson, K.H. (2004). Ribosomal DNA sequence analysis of mucosa-associated bacteria in Crohn's disease. *Inflamm. Bowel Dis.* *10*, 824–833.
- Qin, J., Li, R., Raes, J., Arumugam, M., Burgdorf, K.S.S., Manichanh, C., Nielsen, T., Pons, N., Levenez, F., Yamada, T., et al.; MetaHIT Consortium (2010). A human gut microbial gene catalogue established by metagenomic sequencing. *Nature* *464*, 59–65.
- Qin, J., Li, Y., Cai, Z., Li, S.S., Zhu, J., Zhang, F., Liang, S., Zhang, W., Guan, Y., Shen, D., et al. (2012). A metagenome-wide association study of gut microbiota in type 2 diabetes. *Nature* *490*, 55–60.
- Rao, C.R. (1982). Diversity and dissimilarity coefficients: a unified approach. *Theor. Popul. Biol.* *21*, 24–43.
- Rao, C. (1984). Convexity properties of entropy functions and analysis of diversity. *Lect. Notes-Monograph Ser.* *5*, 68–77.
- Reiter, R.J. (1991). Pineal melatonin: cell biology of its synthesis and of its physiological interactions. *Endocr. Rev.* *12*, 151–180.
- Rinke, C., Schwientek, P., Sczyrba, A., Ivanova, N.N., Anderson, I.J., Cheng, J.-F., Darling, A., Malfatti, S., Swan, B.K., Gies, E.A., et al. (2013). Insights into the phylogeny and coding potential of microbial dark matter. *Nature* *499*, 431–437.
- Sjögren, K., Engdahl, C., Henning, P., Lerner, U.H., Tremaroli, V., Lagerquist, M.K., Bäckhed, F., and Ohlsson, C. (2012). The gut microbiota regulates bone mass in mice. *J. Bone Miner. Res.* *27*, 1357–1367.
- Sonnenburg, J.L., Xu, J., Leip, D.D., Chen, C.-H., Westover, B.P., Weatherford, J., Buhler, J.D., and Gordon, J.I. (2005). Glycan foraging in vivo by an intestine-adapted bacterial symbiont. *Science* *307*, 1955–1959.
- Subramanian, S., Huq, S., Yatsunenko, T., Haque, R., Mahfuz, M., Alam, M.A., Benezra, A., DeStefano, J., Meier, M.F., Muegge, B.D., et al. (2014). Persistent gut microbiota immaturity in malnourished Bangladeshi children. *Nature* *510*, 417–421.
- Wang, M., Song, F., Wu, R., Allen, K.N., Mariano, P.S., and Dunaway-Mariano, D. (2013). Co-evolution of HAD phosphatase and hotdog-fold thioesterase domain function in the menaquinone-pathway fusion proteins BF1314 and PG1653. *FEBS Lett.* *587*, 2851–2859.
- Willing, B.P., Dicksved, J., Halfvarson, J., Andersson, A.F., Lucio, M., Zheng, Z., Järnerot, G., Tysk, C., Jansson, J.K., and Engstrand, L. (2010). A pyrosequencing study in twins shows that gastrointestinal microbial profiles vary with inflammatory bowel disease phenotypes. *Gastroenterology* *139*, 1844–1854.e1.
- Xu, J., and Gordon, J.I. (2003). Honor thy symbionts. *Proc. Natl. Acad. Sci. USA* *100*, 10452–10459.
- Yatsunenko, T., Rey, F.E.E., Manary, M.J.J., Trehan, I., Dominguez-Bello, M.G.G., Contreras, M., Magris, M., Hidalgo, G., Baldassano, R.N.N., Anokhin, A.P.P., et al. (2012). Human gut microbiome viewed across age and geography. *Nature* *486*, 222–227.

Cell Host & Microbe, Volume 17

## **Supplemental Information**

### **Dynamics and Stabilization of the Human Gut Microbiome during the First Year of Life**

Fredrik Bäckhed, Josefine Roswall, Yangqing Peng, Qiang Feng, Huijue Jia, Petia Kovatcheva-Datchary, Yin Li, Yan Xia, Hailiang Xie, Huanzi Zhong, Muhammad Tanweer Khan, Jianfeng Zhang, Junhua Li, Liang Xiao, Jumana Al-Aama, Dongya Zhang, Ying Shiuan Lee, Dorota Kotowska, Camilla Colding, Valentina Tremaroli, Ye Yin, Stefan Bergman, Xun Xu, Lise Madsen, Karsten Kristiansen, Jovanna Dahlgren, and Wang Jun

**Supplemental Information**  
**for**  
**Dynamics and Stabilization of the Human Gut Microbiome**  
**during the First Year of Life**

Fredrik Bäckhed<sup>1,2,\*</sup>, Josefine Roswall<sup>3,4</sup>, Yangqing Peng<sup>5</sup>, Qiang Feng<sup>5,6</sup>, Huijue Jia<sup>5</sup>,  
Petia Kovatcheva-Datchary<sup>1</sup>, Yin Li<sup>5</sup>, Yan Xia<sup>5</sup>, Hailiang Xie<sup>5</sup>, Huanzi Zhong<sup>5</sup>,  
Muhammad Tanweer Khan<sup>1</sup>, Jianfeng Zhang<sup>5</sup>, Junhua Li<sup>5</sup>, Liang Xiao<sup>5</sup>, Jumana  
Al-Aama<sup>5,7</sup>, Dongya Zhang<sup>5</sup>, Ying Shiuan Lee<sup>1</sup>, Dorota Kotowska<sup>6</sup>, Camilla Colding<sup>6</sup>,  
Valentina Tremaroli<sup>1</sup>, Ye Yin<sup>5</sup>, Stefan Bergman<sup>4,8</sup>, Xun Xu<sup>5</sup>, Lise Madsen<sup>6,9</sup>, Karsten  
Kristiansen<sup>5,6</sup>, Jovanna Dahlgren<sup>4,\*,#</sup>, Wang Jun<sup>5,6,7,10,11\*,#</sup>

**Content:**

Extended Experimental Procedures

Supplemental References

Supplemental Figure Legends

List of Supplemental Tables

# Extended Experimental Procedures

## Study population and sampling

Out of the 98 recruited children, all except three had complete fecal sampling series (3 newborn samples missing, 2 vaginally born, 1 C-section). All infants were included in the comparison between vaginal delivery and C-section for microbiota composition and determination of signature genera/MetaOTUs (n=83 vs n=15), while only the 83 vaginally delivered infants were included in the functional comparisons, and MetaOTU networks. Parents were asked to fill in questionnaires regarding pregnancy data and feeding practices during first week and at 4 and 12 months of age. Antibiotic usage was collected from medical records (hospital treatment) and from the Swedish national prescription register (open clinic treatment). For detailed description of the study population see Table 1. Among the 98 infants included in this study, 15 were delivered by cesarean section. The C-section rate among full term infants in Halland during the inclusion period was 17.8%.

Among C-section delivered infants, all mothers except of 3 were in active labor with rupture of membranes when the decision of caesarian was made. The reason for cesarean delivery ranged from failure of induction (n=2) bad progress of labor (n=4), disproportion (n=3), breech/abnormal fetal position (n=2) to asphyxia of the child (n=4).

## **Antibiotic treatment**

Mothers (13/98 of mothers; 10/83 of mothers delivering vaginally and 3/15 of mother delivered by C-section) with fever or colonized by group B streptococcus were given antibiotics (12 Benzyl penicillin 3g x 1-4 iv, 1 clindamycin 900 mg x 1 iv, ranging from 24h to 50 minutes before delivery) at the ward before delivery. None of the mothers who delivered vaginally (n=83) received antibiotics during delivery. The majority of mothers delivering through C-section, (10/15) were given a single dose of prophylactic antibiotics per operative after the delivery of the child according to local routines (8 Piperacillin /Tazobaktam 4 g iv , 2 Clindamycin 600mg iv).

Among the infants 2/98 were given intravenous (iv) antibiotics during the immediate neonatal period and another 3/98 children received antibiotics before 4 months of age. All except one were given iv broad-spectrum antibiotics for bacterial infections. 23/98 children received antibiotics between 4 and 12 months of age, mainly oral antibiotics for upper airway and middle ear infections. 60 % of the children treated with antibiotics from 4-12 months of age received fenoximetylpencillin. 6/24 children were treated with antibiotics repeatedly between 4 and 12 months of age (4 children 2 times and 2 children 3 times)

## **Feeding patterns**

During first week of life 88 % of parents reported feeding practices and among them 74.4% of mothers reported exclusive breast feeding, 24.4% mixed feeding and 1.2 % exclusive formula feeding. At 4 months of age all except 2 parents completed

feeding practices questionnaires and among them, 68.8% were exclusively breast-fed, 19.8 % were given a mix of breast milk and formula, whereas 11.4% were exclusively formula fed (all but one were provided NAN formula). 25,3% of the study infants had started with taste portions at 4 months of age. At 12 months of age 14% of the children were still provided some degree of breast feeding.

### ***De novo* assembly of contigs and genomes**

To determine the best index for assembling high-quality reads into contigs (Luo et al., 2012), we tested the k-mer length ranging from 31bp to 49 bp by 2 bp for each sample. The longest assembly was selected as the assembled contig set and was used for constructing species catalogs and gene catalogs. We evaluated how well the assembled contigs represented the information captured from sequencing by aligning the reads back to the contig sets. We could align  $92.59\% \pm 4.51\%$  for newborns,  $91.40\% \pm 4.32\%$  for 4 month-old infants,  $89.82 \pm 3.21\%$  for 12 month-old infants, and  $79.32\% \pm 5.08\%$  for mothers.

The contigs were divided into three categories to reconstruct all genomes from each infant sample: 1) Contigs that map to known genomes in the NCBI bacteria/archaea genome database (version 2011-08) with a BLAST score of more than 200 and >70% overlap were binned according to the known genomes; 2) Unknown contigs with a sequencing depth of at least 20X were binned according to abundance co-variations as explained in the following paragraph; 3) Unknown contigs with a sequencing depth of less than 20X were subject to hierarchical clustering

(hclust) based on Kendall's correlation coefficient and only clusters with greater than 100 contigs were further considered as a bin.

For the 2<sup>nd</sup> category, we assumed that the relative abundance of sequences from the same strain will co-vary across all samples (Qin et al., 2012). Accordingly, we sorted the contigs into tentative genome bins: 1) we first estimated relative abundance profiles for contigs assembled from one sample across all samples and calculated the pairwise kendall tau correlation coefficients between contigs according to the relative abundance profiles; 2) we next clustered the closely related contigs into bins according to pairwise correlation coefficients using an Ordering Points to Identify the Clustering Structure (OPTICS) clustering method.

For all bins, we then used the clustering result as input for an Expectation-Maximization (EM)-based cluster optimization. Finally, we manually separated sequences in a bin if more than one cluster could be identified in the GC content vs. depth of coverage graph. Thereafter were sequencing reads from each sample aligned to the contigs within each bin. The pool of reads retrieved were reassembled using SOAPdenovo2 (Luo et al., 2012) for optimal assembly.

Using this protocol, we in total obtained 4356 genomes with genome size over 0.9Mbp from the infant samples. On average 6.4 genomes/per sample were assembled from first week newborns' microbiome, 11.7 genomes per sample for 4 month infants' microbiome and 25.9 genomes per sample for 12 month infants' microbiome. We avoided performing binning on the assembled result of the mothers' samples because of the higher complexity of the adult gut microbiome (Table S2).

## **Construction of MetaOTUs and taxonomic assignments**

We included genomes from NCBI bacteria/archaea genome database (version 2011-08) into our recovered genome set. To avoid introducing non-intestinal microbial genomes into our dataset, we mapped all of our contigs to NCBI bacteria/archaea genome database, and selected the genome with cut-off > 5% (threshold for a hit:  $10^{-5}$ ). As a result, in total 1147 genomes/draft genomes are introduced into our recovered genome set for OTU clustering.

OTU clustering were based on genome-genome distance measured with a simplified version of MUMi (Deloger et al., 2009) and the Spearman distance (Leung et al., 2011). MUMi value is a relatively direct measurement of DNA sequence identity, and it performs well when either of the two genomes in comparison is of high completeness. However it tends to overestimate the genome-genome distance when neither of the genomes is complete. Thus we used Spearman distance as a complement. Spearman distance is a method of measuring similarity of the 4-mer frequency of DNA sequences, based on the assumption that sequences derived from the same genome/species tend to have a more similar 1-mer frequency distribution than DNA sequences from two different genomes/species (Chor et al., 2009). We clustered the genomes into OTUs in a two-step sub graph searching method: first we used MUMi values as rigorous criteria to clustered genomes into preliminary OTU, 2) then use Spearman Distance to cluster the preliminary OTUs that are mistakenly separated due to genome incompleteness. We constructed a network with 5141

genomes as nodes and connected genomes based on their similarity, and identified subclusters with connectivity  $>0.5$  using a hierarchical agglomerative clustering technique.

To estimate the best threshold (minimum combination similarity) of OTU clustering, we performed a simulation using the 1147 genomes from NCBI database. We use rand index (Rand, 1971) as the measurement of similarity between the clustering results and the real taxonomic classifications. By optimizing the rand index, we observed the best threshold for generating a species level MetaOTU at around 0.54~0.55 for MUMi and around 300-400 for Spearman Distance.

Using this protocol and the minimum combination similarity of 0.54 for MUMi and 300 for (Spearman Distance), we generated 690 MetaOTU that are closest to the species level taxonomic assignment. The taxonomic assignment of each MetaOTU is determined by the taxonomic information of the NCBI retrieved genomes that resided within the OTU. 317 out of 690 MetaOTU (45.9%) are novel OTUs with no known species associated. Among the 373 known MetaOTUs, 323 MetaOTUs (86.6%) are assigned to single species/strains, whereas 368 MetaOTUs (98.7%) are assigned to single genus (Table S2). This MetaOTU catalog is highly representative for our sample: the reads usage rate are  $95.90\% \pm 4.71\%$  for first week newborns,  $94.69\% \pm 5.15\%$  for 4 month infants,  $94.62\% \pm 2.96\%$  for 12M infants, and  $75.00\% \pm 11.11\%$  for mothers.

### **Genome-genome distance estimated with MUMi**

Two genomes a and b are first aligned to each other using MUMmer 3.22 (Kurtz et al., 2004) with parameter  $-b -c -l 17$ , generating the MUM list. MUMi value (Deloger et al., 2009) is then computed using the MUM list as following

$$MUMi = 1 - \frac{L_{unmap\ length\ of\ a} + L_{unmap\ length\ of\ b}}{L_{total\ length\ of\ a} + L_{total\ length\ of\ b}}$$

MUMi value is a similarity value, where MUMi close to 1 means very similar genomes, whereas MUMi close to 0 are obtained from distant genomes.

### Estimation of relative abundance of genome/MetaOTU/gene/KO

*MetaOTU relative abundance estimation:*

Using 90% identity as threshold, we removed the redundant genomes and used the longest genome as the representative genome for the group, resulting in 3606 genomes groups. Thereafter we used SOAPaligner (<http://soap.genomics.org.cn/soapaligner.html>) to align reads back to these 3606 genomes (90% identity as threshold for a hit, multiple hits are all kept) and estimated the relative abundance of each genomes using:

$$Depth(g_i) = \begin{cases} \frac{\sum_{j \in A_1} a_j}{L_1 + L_0} & \dots \dots \dots \text{if } \frac{L_2}{L_2 + L_0} > 0.005 \\ 0 & \dots \dots \dots \text{if } \frac{L_2}{L_2 + L_0} < 0.005 \end{cases}$$

$$\text{Relative abundance}(p_i) = \frac{g_i}{\sum_{i=1}^N g_i} \quad (\text{in total } N \text{ genomes within a sample})$$

$g_i$ : the depth of genome  $i$

$p_i$ : the relative abundance of genome  $i$

$a_j$ : the depth of coverage of base-pair  $j$

$A_1$ : the set of base-pairs that are unique to genome  $i$  (the reads that are only aligned

to this genome)

$A_2$ : the set of base-pairs that are covered by at least one read

$A_0$ : set of base-pairs that are not covered by any reads.

$L_0$ : The number of base-pairs that are not covered by any reads.

$L_1$ : The number of base-pairs that are unique to genome  $i$

$L_2$ : The number of base-pairs that are covered by reads.

The relative abundance of MetaOTUs is estimated by summing relative abundance of genomes that belong to the same OTU and renormalizing to one.

*Genus/phylum relative abundance estimation*: is estimated by adding the relative abundance of MetaOTUs that belong to the same genus/phylum and then normalize to one. Note that when profiling genus/phylum, the novel MetaOTU are not taken into account.

*Gene relative abundance estimation*: as described previously (Qin et al., 2012).

*KO relative abundance estimation*: KO relative abundance is estimated by summing relative abundance of genes annotated to KO and renormalizing to one.

### **Decomposition of community diversity**

We employed the quadratic entropy proposed by Rao (Rao, 1982) as the measure of diversity and performed the decomposition of the community diversity

(total quadratic entropy) in a way similar to ANOVA (Rao, 1984) so that the total quadratic entropy of a community (gamma-diversity) can be decomposed into within-sample entropy (alpha-diversity) and between-sample entropy (beta-diversity). The method allowed us to take into account both the species-species taxonomic distance and the relative abundance into the diversity analysis. When performing diversity analysis on MetaOTU profile, we used the averaged pairwise genome-genome MUMi between two MetaOTU as the MetaOTU-MetaOTU distance. When performing diversity analysis with genus profile or KO profile, all genus-genus/KO-KO distances were considered to be 1. This analysis is implemented with the 'ade4' package of R (Pavoine et al., 2004).

### **MetaOTU-based UniFrac distance estimation**

UniFrac distance was first proposed to “measures the distance between communities based on the lineages they contain” in the context of 16S rRNA sequence analysis (Lozupone and Knight, 2005). In our study we used the exact way to compute unweighted UniFrac distance as the measure of sample-sample similarity with the MetaOTU-based phylogenetic tree. MetaOTU-MetaOTU distance was measured by averaging all pairwise genome-genome MUMi between two MetaOTU. We used the MetaOTU distance matrix as input to build a phylogenetic tree with neighbor-joining method and used midpoint method of rooting the tree with 'freetree' program. We next used a customized script to compute the UniFrac distance from the distance information between nodes of the tree files. The relative abundance profile of

MetaOTUs was used to determine the presence or absence of each MetaOTU (i.e., all genomes in the MetaOTU have  $L_2/(L_2+L_0) < 0.005$ ).

Other methods to measure sample-sample distance used in this study include a probability distribution distance metric related to Jensen-Shannon divergence (JSD) (Arumugam et al., 2011) , Bray–Curtis dissimilarity (Bray and Curtis, 1957) that are all computed using customized scripts following the method proposed in the paper.

### **Identification of signature genera/MetaOTUs**

We used IndVal, an index widely used in ecology (Dufrene and Legendre, 1997), to assess species-habitat associations. To identify signature genera/MetaOTUs for each habitat, IndVal was calculated as

$$IndVal_{ind} = \frac{a_p}{a} \times \frac{n_p}{N_p}$$

$a_p$ : sum of the abundance values of the species within the target site group

$n_p$ : number of occurrences of the species within the target site group

$a$ : sum of the abundance values of the species over all sites

$N_p$ : number of sites belonging to the target site group

Random permutation of relative abundance of each genus/MetaOTU across communities was performed 199 times, and after each permutation, IndVal (the preference of the species for the target habitat) was recalculated. We used the highest IndVal to determine which specie is associated with the site group and the p-value of the permutation test (the test of positive species preference) as the proportion of permutations that yielded the same or higher IndVal as observed for the

unpermuted data. In each permutation, the highest IndVal among the site groups (not necessarily the site group before permutation) was used for statistical testing in order to avoid multiple testing.

### **Reporter score for pathways/modules**

We used a reporter feature algorithm (Patil and Nielsen, 2005) to identify KEGG pathways or modules enriched in a cohort relative to another. One-tail Wilcoxon rank-sum test was performed on all the KOs that occurred in more than 5 samples and adjusted for multiple testing (Benjamini et al., 1995). The Z-score for each KO could then be calculated:

$$Z_{KO_i} = \theta^{-1}(1 - p_{KO_i})$$

where  $\theta^{-1}$  is the inverse normal cumulative distribution,  $p_{KO_i}$  is the adjusted p-value for that KO. The aggregated Z-score for a KEGG pathway (or module) is then:

$$Z_{pathway} = \frac{1}{\sqrt{k}} \sum Z_{KO_i}$$

where k is the number of KOs involved in the pathway (or module).

We corrected the background distribution of  $Z_{pathway}$  by subtracting the mean ( $\mu_k$ ) and dividing by the standard deviation ( $\sigma_k$ ) of the aggregated Z-scores of 1000 sets of k KO, chosen randomly from the whole metabolic KO network:

$$Z_{adjusted\ pathway} = \frac{Z_{pathway} - \mu_k}{\sigma_k}$$

The  $Z_{adjusted\ pathway}$  was used as the final reporter score for evaluating the enrichment of specific pathways or modules. A reporter score=1.6 (90% confidence according to normal distribution) was used as the detection threshold for significantly

differentiating pathways.

## **Statistical analysis of influencing factors**

### **Determine the factors' significance of influence (PERMANOVA)**

PERMANOVA is implemented with a modified version of 'adonis' in R. The test is performed on each influencing factor respectively with 9999 permutations.

### **Determine percentage of variation explained by each factors**

Percentages of variation of a species data matrix explained by each influencing factor are estimated by performing constrained analysis of principal coordinates to every factor respectively. Constrained analysis of principal coordinates (Anderson and Willis, 2013) is an ordination method similar to redundancy analysis, but allow for non-Euclidean distance matrix. These analyses are performed using the function `capscale` in the 'vegan' package in R.

### **Effect size of influencing factors**

Effect size, a descriptive statistic that conveys the estimated magnitude of a relationship was calculated using Cohen's  $d$ , the difference between two means divided by a standard deviation for the data:

$$d = \frac{\bar{x}_1 - \bar{x}_2}{s}$$

$s$ , the standard deviation, is calculated as a pooled standard deviation with two independent populations as:

$$s = \sqrt{\frac{(n_1 - 1)s_1^2 + (n_2 - 1)s_2^2}{n_1 + n_2 - 2}}$$
$$s_1^2 = \frac{1}{n_1 - 1} \sum_{i=1}^{n_1} (x_{1,i} - \bar{x}_1)^2$$

$\bar{x}_1, \bar{x}_2$ : Means of two populations.

$n_1, n_2$ : Number of samples of two populations.

$s_1, s_2$ : Standard deviations of two populations

We computed Cohen's d effect size for all genera that occurred in more than 10 samples, and for all MetaOTU that occurred in more than 5 samples.

## Supplemental References

Anderson, M.J., and Willis, T.J. (2013). Canonical Analysis of Principal Coordinates: A Useful Method of Constrained Ordination for Ecology. *CANONICAL ANALYSIS OF PRINCIPAL COORDINATES: A USEFUL METHOD OF CONSTRAINED ORDINATION FOR ECOLOGY*. *Ecology* *84*, 511–525.

Arumugam, M., Raes, J., Pelletier, E., Le Paslier, D., Yamada, T., Mende, D.R., Fernandes, G.R., Tap, J., Bruls, T., Batto, J.-M., et al. (2011). Enterotypes of the human gut microbiome. *Nature* *473*, 174–180.

Benjamini, Y., Hochberg, Y., Yoav Benjamini, and Hochberg, Y. (1995). Controlling the False Discovery Rate: A Practical and Powerful Approach to Multiple Testing. *J. R. Stat. Soc. Ser. B* *57*, 289–300.

Bray, J., and Curtis, J. (1957). An ordination of the upland forest communities of southern Wisconsin. *Ecol. Monogr.* *27*, 325–349.

Chor, B., Horn, D., Goldman, N., Levy, Y., and Masingham, T. (2009). Genomic DNA k-mer spectra: models and modalities. *Genome Biol.* *10*, R108.

Deloger, M., El Karoui, M., and Petit, M.-A. (2009). A genomic distance based on MUM indicates discontinuity between most bacterial species and genera. *J. Bacteriol.* *191*, 91–99.

Dufrene, M., and Legendre, P. (1997). SPECIES ASSEMBLAGES AND INDICATOR SPECIES: THE NEED FOR A FLEXIBLE ASYMMETRICAL APPROACH. *Ecol. Monogr.* *67*, 345–366.

Kent, W.J. (2002). BLAT--the BLAST-like alignment tool. *Genome Res.* *12*, 656–664.

Kurtz, S., Phillippy, A., Delcher, A.L., Smoot, M., Shumway, M., Antonescu, C., and Salzberg, S.L. (2004). Versatile and open software for comparing large genomes. *Genome Biol.* *5*, R12.

Leung, H.C.M., Yiu, S.M., Yang, B., Peng, Y., Wang, Y., Liu, Z., Chen, J., Qin, J., Li, R., and Chin, F.Y.L. (2011). A Robust and Accurate Binning Algorithm for Metagenomic Sequencing. *Bioinformatics* *27*, 1489–1495.

Lombard, V., Golaconda Ramulu, H., Drula, E., Coutinho, P.M., and Henrissat, B. (2014). The carbohydrate-active enzymes database (CAZy) in 2013. *Nucleic Acids Res.* *42*, D490–D495.

- Lozupone, C., and Knight, R. (2005). UniFrac: a new phylogenetic method for comparing microbial communities. *Appl. Environ. Microbiol.* *71*, 8228–8235.
- Luo, R., Liu, B., Xie, Y., Li, Z., Huang, W., Yuan, J., He, G., Chen, Y., Pan, Q., Liu, Y., et al. (2012). SOAPdenovo2: an empirically improved memory-efficient short-read de novo assembler. *Gigascience* *1*, 18.
- Patil, K.R., and Nielsen, J. (2005). Uncovering transcriptional regulation of metabolism by using metabolic network topology. *Proc. Natl. Acad. Sci. U. S. A.* *102*, 2685–2689.
- Pavoine, S., Dufour, a-B.A.-B., and Chessel, D. (2004). From dissimilarities among species to dissimilarities among communities: a double principal coordinate analysis. *J. Theor. Biol.* *228*, 523–537.
- Qin, J., Li, Y., Cai, Z., Li, S.S., Zhu, J., Zhang, F., Liang, S., Zhang, W., Guan, Y., Shen, D., et al. (2012). A metagenome-wide association study of gut microbiota in type 2 diabetes. *Nature* *490*, 55–60.
- Rand, W. (1971). Objective criteria for the evaluation of clustering methods. *J. Am. Stat. Assoc.* *66*, 846–850.
- Rao, C. (1984). Convexity properties of entropy functions and analysis of diversity. *Lect. Notes-Monograph Ser.* *5*, 68–77.
- Rao, C.R. (1982). Diversity and dissimilarity coefficients: a unified approach. *Theor. Popul. Biol.* *21*, 24–43.
- Rinke, C., Schwientek, P., Sczyrba, A., Ivanova, N.N., Anderson, I.J., Cheng, J.-F., Darling, A., Malfatti, S., Swan, B.K., Gies, E.A., et al. (2013). Insights into the phylogeny and coding potential of microbial dark matter. *Nature*.
- Subramanian, S., Huq, S., Yatsunenko, T., Haque, R., Mahfuz, M., Alam, M. a., Benezra, A., DeStefano, J., Meier, M.F., Muegge, B.D., et al. (2014). Persistent gut microbiota immaturity in malnourished Bangladeshi children. *Nature* *509*, 417–421.

# Supplemental Figure Legends

## **Figure S1 Organizing the gut microbiome into MetaOTUs. (Related to Fig. 1)**

Diagram for construction of the gene catalogs, genome assemblies and MetaOTUs. Metagenomic shotgun sequencing reads were assembled into contigs using SOAPdenovo2 (Luo et al., 2012). The contigs were binned according to their abundance variations across samples, and GC-depth pattern, for further assembly into draft genomes. The draft genomes, together with available bacterial and archaeal genomes from NCBI that could be identified in our metagenomes (>5% coverage by contigs), were then clustered into MetaOTUs based on MUMi (Deloger et al., 2009) and the Spearman distance (Leung et al., 2011), and their taxa were determined in relation to the NCBI genomes. For construction of the gene catalogs, genes were predicted from the assembled contigs and redundant genes were removed using BLAT (Kent, 2002) (90% overlap, 95% identity).

## **Figure S2 Differences in the composition and dynamics of the fecal microbiota between vaginally and C-section delivered infants during the first year of life. (Related to Fig. 2)**

**(A,B,C)** Box plots for within- and between-group Bray's distance for the naturally or C-section born infants and their mothers at the genus **(A)** and MetaOTU **(B)**. Red: vaginally born; green: C-section; blue: between vaginally born and C-section.  $p < 2.2e-16$  for all. Wilcoxon rank-sum test. **(C)** Influence of sampling time on the most abundant genus in newborns ( $n=98$ ). Box-and-whisker plot for age distribution. Kruskal-Wallis test  $p=3.131e-4$  among the three groups. \*\*:  $p < 0.01$ , Wilcoxon rank-sum test between groups.

## **Figure S3 Dynamics of functional modules in vaginally delivered first-year infants. (Related to Fig. 3)**

**(A)** Box plot for distance between infants and mothers and scatter plot from PCoA, based on unweighted UniFrac distance at KO levels. **(B)** Box plot for relative abundance of pectinase in the four cohorts. **(C)** Box plot for relative abundance of *B. thetaiotaomicron* in the four cohorts. NS: Not significant, \*:  $p < 0.05$ , \*\*:  $p < 0.01$ , \*\*\*:  $p < 0.001$ . Wilcoxon ranked sum test. **(D)** Reporter score bar-plots for KO modules involved in carbohydrate metabolism. **(E)** Prevalence of methane-producing or sulfur-reducing bacteria in different stages of infancy.  $n=81$  for newborns,  $n=83$  for 4M, 12M and mothers. **(F,G,H,I)** Reporter score bar-plots for KO modules involved in nitrogen, methane, or sulfur metabolism **(F)**, modules or pathways for cofactor and vitamin metabolism **(G,H)**, and modules for heme and hemin transporters **(I)** ( $n=81$  for newborns,  $n=83$  for 4M, 12M and mothers). Only modules with more than 40% of KOs found in the metagenomes are shown. Dashed lines represent the reporter score of 1.6, the threshold for a significant difference used in such analyses.

**Figure S4 Antibiotic resistance in the infants metagenome (related to Figure 3).**

**(A)** Number of resistance types according to the Antibiotic Resistance Genes Database (ARDB) (Liu and Pop, 2009) in vaginally born neonates (n = 81), 4-month-olds (n = 83), 12-month-olds (n = 83) and mothers (n = 83), with or without antibiotic treatment between 4 and 12 months. **(B)** Average number of resistance types per sample for the vaginally born infants and mothers. **(C)** Occurrence frequency of different antibiotic resistant types in the vaginally born delivered infants and mothers. **(D)** Fraction of resistance genes over the total count of microbial genes in each sample. Box-and-whisker plot. Red: C-section; green: vaginally born. Wilcoxon rank-sum test,  $p=0.027$  between newborns,  $p=0.161$  between 4-month-olds,  $p=0.088$  between 12-month-olds,  $p=0.099$  between mothers.

**Figure S5 Random forest model for microbiota age. (Related to Fig. 6)**

**(A)** Decrease in cross-validation error with increasing number of MetaOTUs considered in the model, similar to (Subramanian et al., 2014). The model was trained with the training set (n=49, vaginally delivered, exclusively breast-fed at newborn and no longer breast-fed at 12M, Fig. 4A). Permutational importance of each MetaOTU is listed in Table S7. Using the relative abundances 137 MetaOTUs shows the lowest cross-validation error, which is 1806.4. We used 64 MetaOTUs, corresponding to a cross-validation error of 1940.0. **(B)** Microbiota age versus chronological age in a test set comprised of C-section delivered infants (n=14 for newborn, n=15 for 4M and 12M). See also Table S7.

# Supplemental Tables

**Table S1 Characteristics of each infant at each sampling point.**  
(Related to Table 1)

**Table S2 Statistics for the sequencing data, gene catalogs, genomes and MetaOTUs annotation of all samples. (Related to Fig. 1)**

\* Number of KO in the modified KEGG KO catalog=9809, i.e. with plant and animal KOs removed.  $\pm$  one standard deviation.

\* SCG, 139 single-copy genes conserved in bacteria, as in (Rinke et al., 2013).

**Table S3 Differentially taxon distribution patterns between delivery modes for newborns, 4-month-old and 12-month-old infants, and mothers. (Related to Fig. 2)**

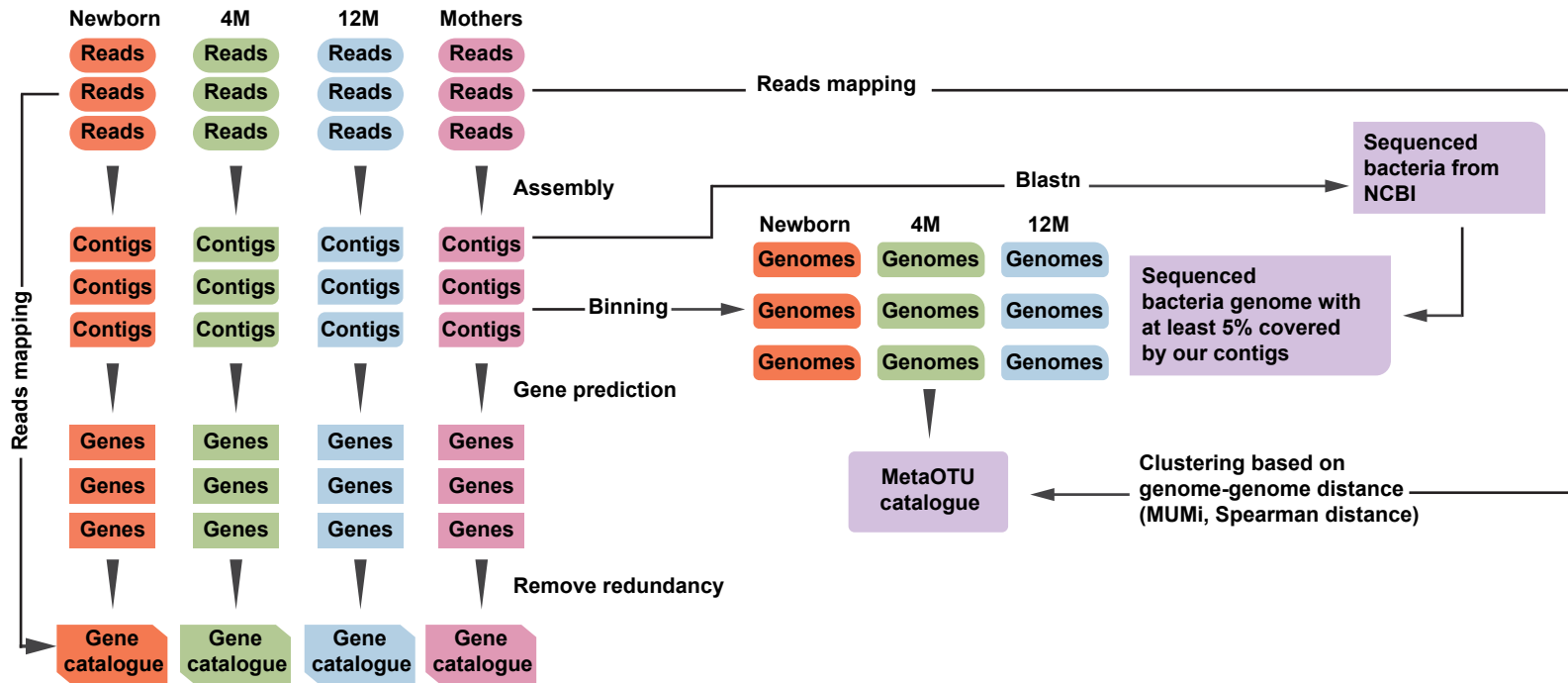
Wilcoxon rank sum test. n=14 C-section vs. 81 vaginally born for newborns; n=15 C-section vs. 83 vaginally born at 4M, 12M and mothers.

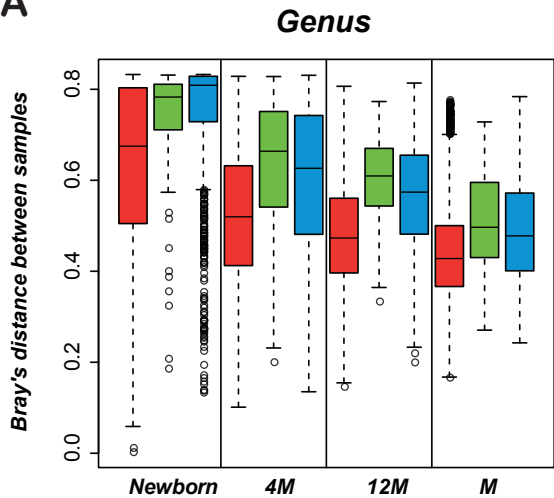
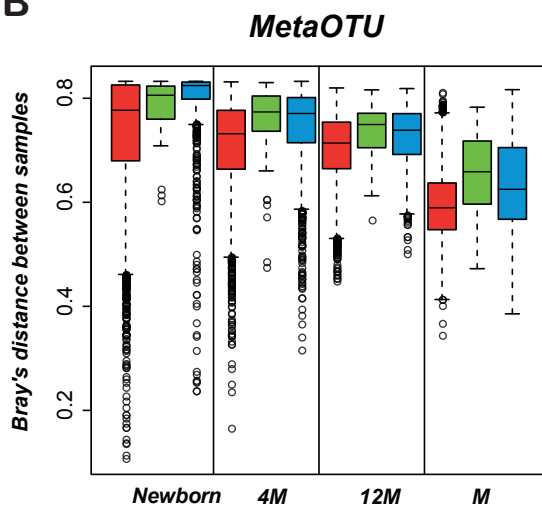
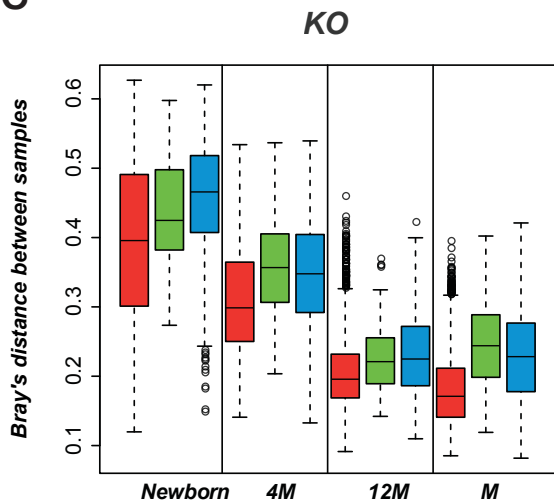
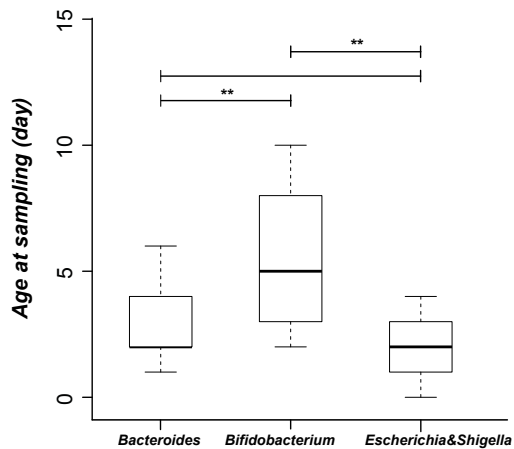
**Table S4 Reporter scores of KO pathways for group comparisons and Spearman's correlation between the vitamin K2 synthesis module and genera.**  
(Related to Fig. 3)

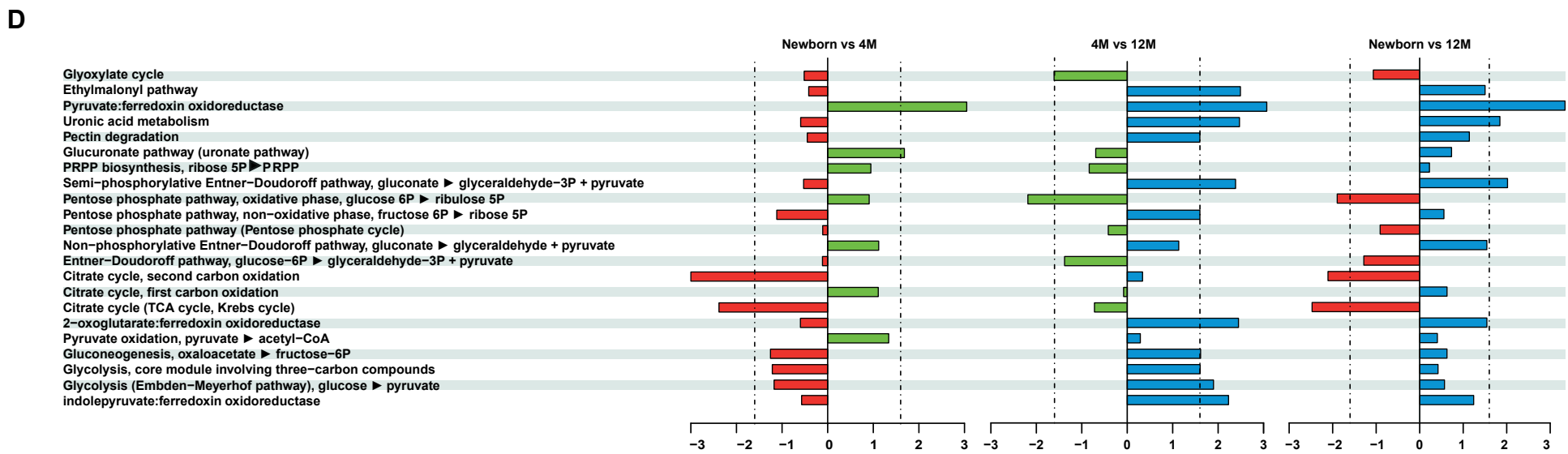
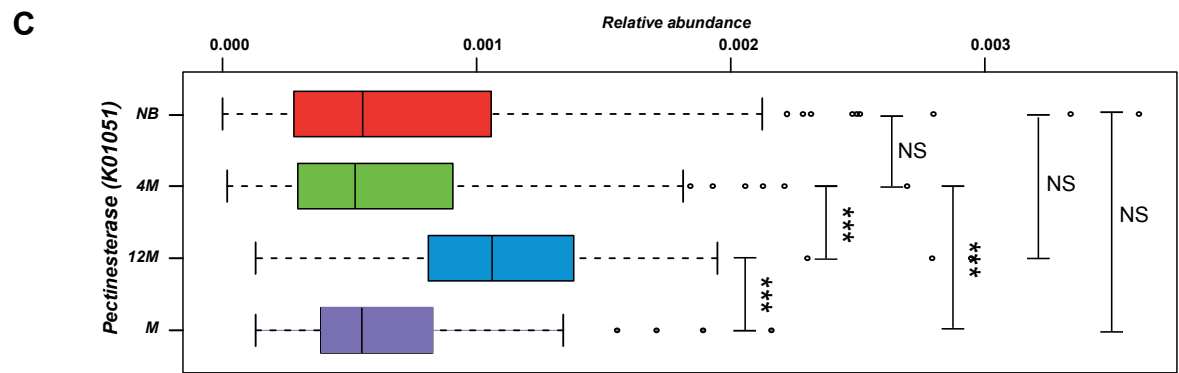
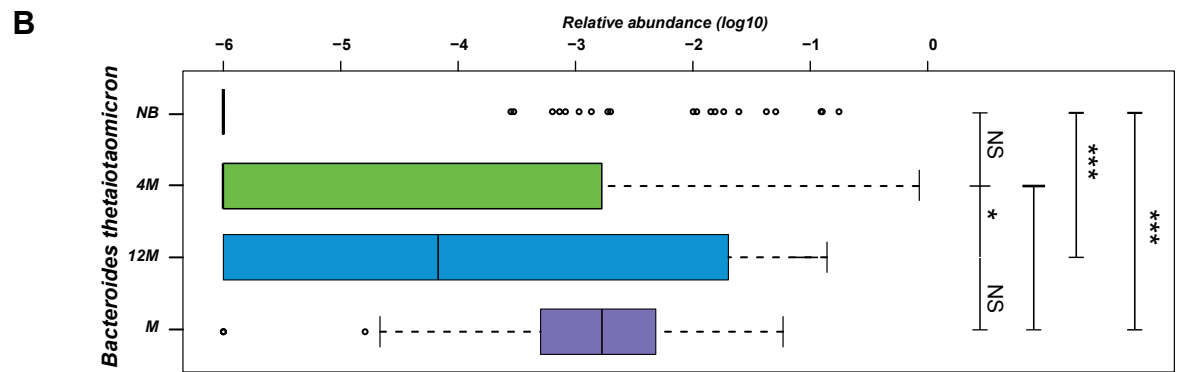
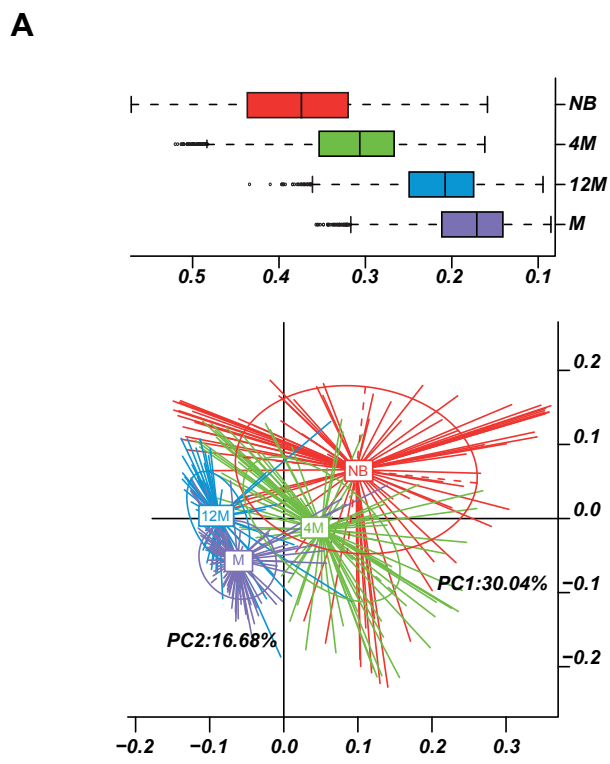
**Table S5 Signature taxons (genera or MetaOTUs) at each stage for infants with different modes of delivery. (Related to Fig. 4)**

**Table S6 Significantly changed MetaOTU network between vaginally delivered infants with different time points. (Related to Fig. 5)**

**Table S7 Statistics for gut microbiota age and feeding pattern on genera and MetaOTUs.(Related to Fig. 6, Fig. S5)**

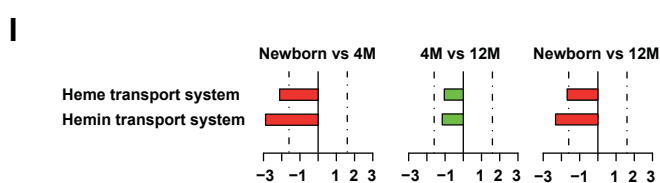
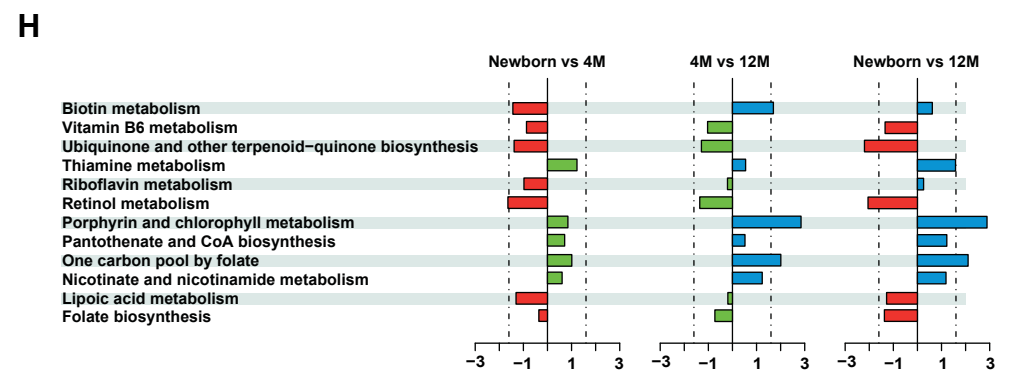
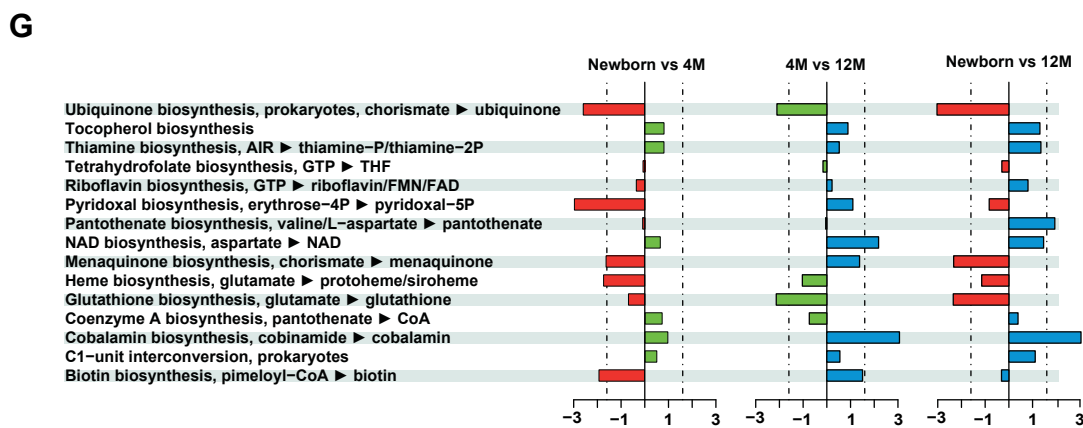
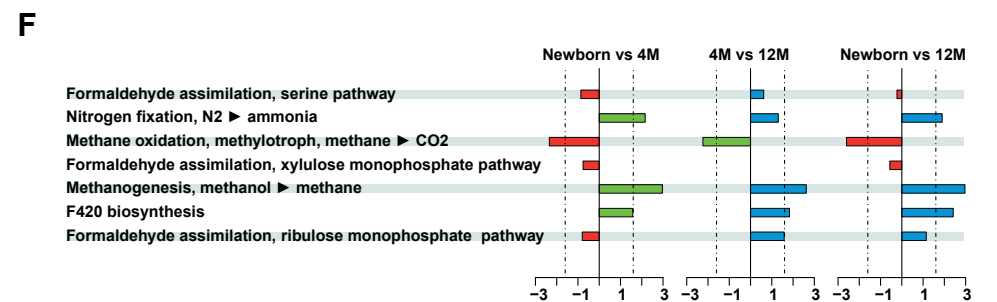


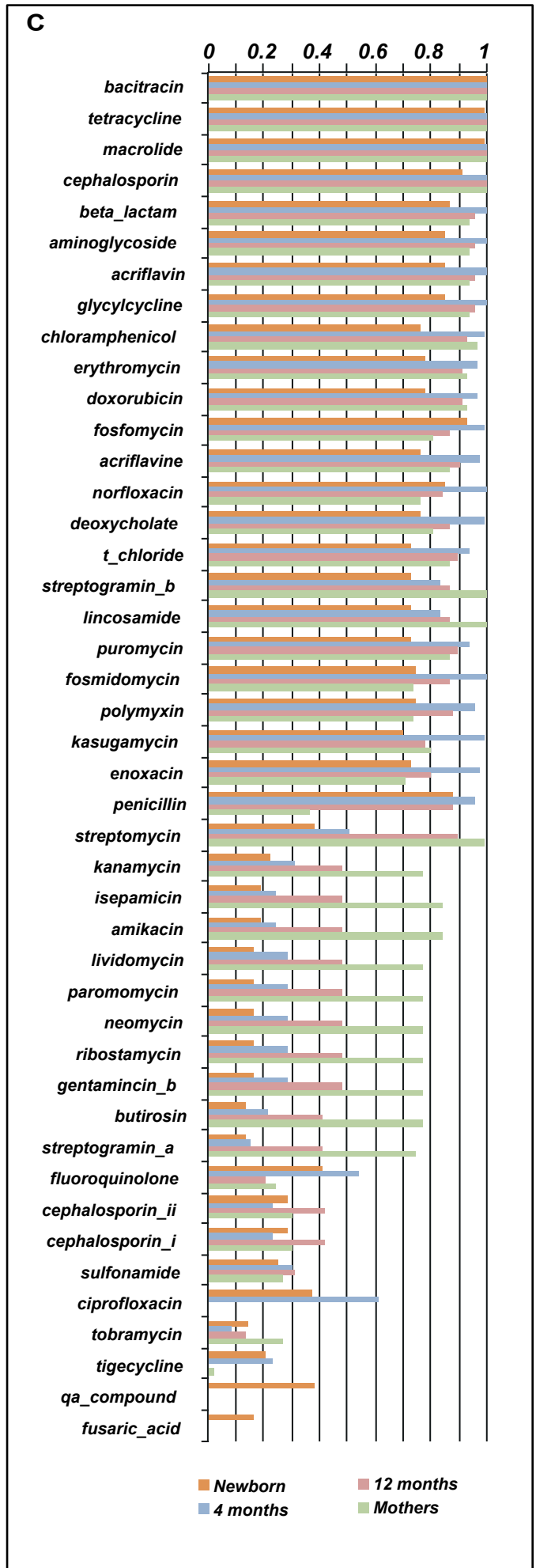
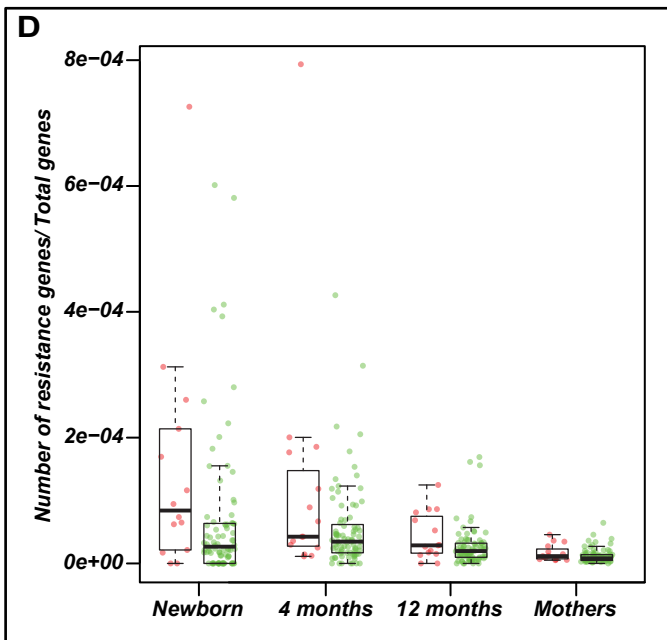
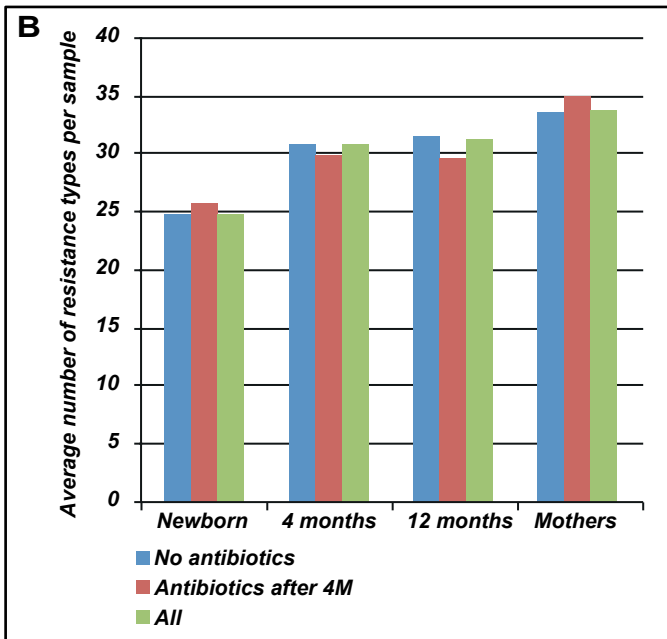
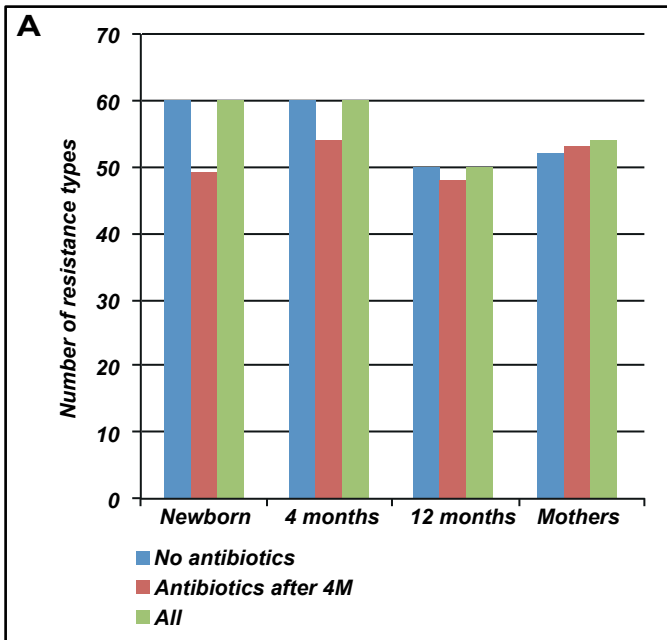
**A****B****C****D**

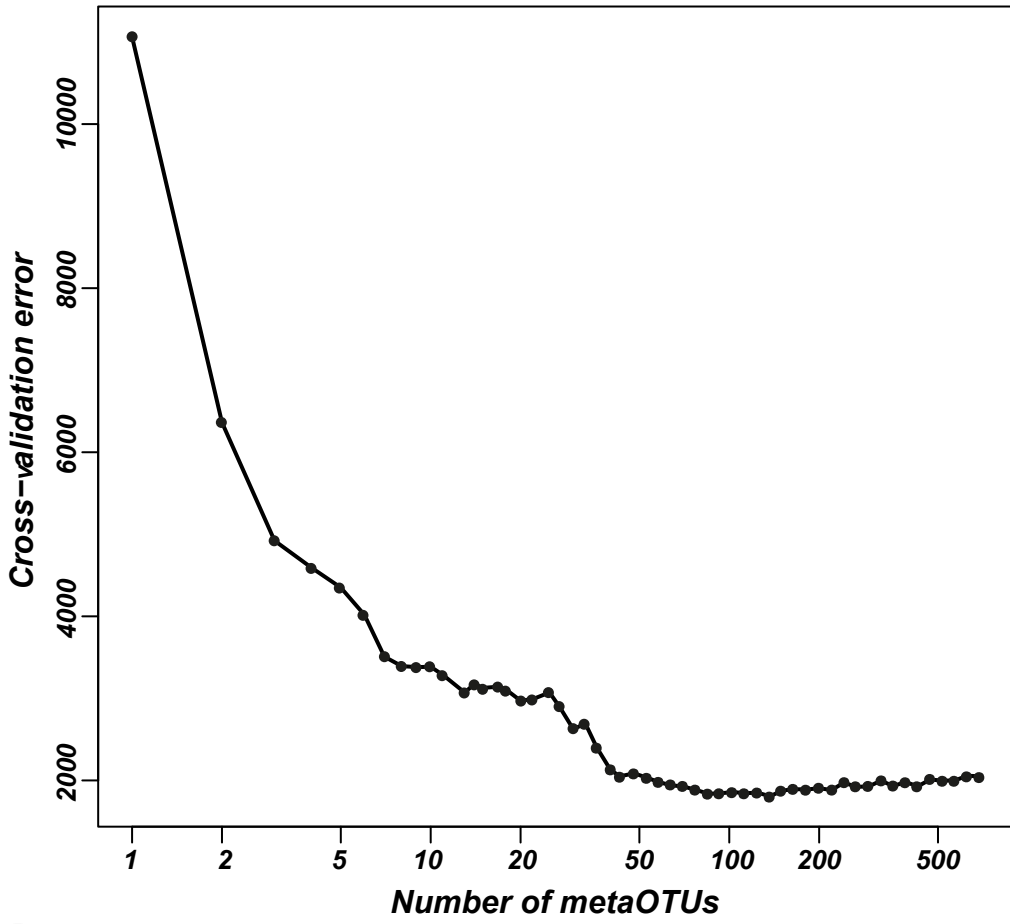


**E**

	Newborn	4M	12M	Mothers
<i>Methanobrevibacter smithii</i>	0	0	2	23
<i>Methanosphaera stadtmanae</i> 07	0	0	0	1
<i>Desulfovibrio vulgaris</i>	0	0	0	0
<i>Desulfovibrio piger</i>	0	0	2	20
<i>Desulfovibrio desulfuricans</i> ATCC 27774 uid59213	0	0	0	1
<i>Desulfovibrio desulfuricans</i> G20 uid57941	0	1	1	2
<i>Desulfovibrio</i> sp1	0	0	1	8





**A****B**